



The preparation, stability and heat-collection efficiency of solar nanofluids

Fengjiao Zhou¹ · Liu Yang¹ · Lei Sun¹ · Songyang Wang¹ · Jianzhong Song² · Xiaoke Li³

Received: 19 June 2022 / Accepted: 15 October 2022 / Published online: 16 December 2022
© Akadémiai Kiadó, Budapest, Hungary 2022

Abstract

The energy crisis and environmental pollution have forced humanity to look for alternative and clean energy. Collecting solar energy by using solar nanofluids (NFs) due to their excellent photo-thermal properties has been popular. Since many literature focused on solar collectors rather than solar nanofluids, this paper was written to promote the commercialization of solar NFs by reviewing state-of-the-art advances in the preparation techniques, stability, and heat-collection efficiency of solar NFs. The first procedure is to prepare stable NFs, and the preparation techniques of NFs were briefly evaluated, including the one-step method, two-step method, post-treatment method, and phase transfer method. Then, the stability mechanism of NFs was elucidated from a microscopic perspective and the effect of the dielectric constant of base fluid, pH value, surfactant, the size, shape, and concentration of nanoparticles on the stability of NFs were explored. The heat-collection efficiency of solar NFs was also discussed. It is found that the unique optical properties of solar NFs effectively/significantly improved the absorption of solar radiation; meanwhile, the high thermal conductivity (TC) of solar NFs can also improve the efficiency of conversion and transmission of solar collectors. Finally, the knowledge gap and future challenges of solar NFs are summarized, and corresponding suggestions are put forward, hoping to promote the process of putting solar NFs into collectors for commercial use officially.

Keywords Solar nanofluids · Preparation · Stability · Heat collection

Abbreviations

NFs	Nanofluids
TC	Thermal conductivity
CNTs	Carbon nanotubes
EG	Ethylene glycol
PWE	Pulsed-wire evaporation
EEW	Electro-explosive wire
DW	Distilled water
NHS	N-hydroxysuccinimide
SDBS	Sodium dodecylbenzenesulfonate
CTAB	Cetyltrimethylammonium bromide

SDS	Sodium dodecylsulfate
IEP	Isoelectric point
TX-100	Triton X-100
GA	Gum Arabic
TEM	Transmission electron microscope
DLS	Dynamic light scattering
TGA	Thermo-gravimetric analysis
MWCNT	Multi-walled carbon nanotubes

Symbols

V	Velocity of nanoparticles ($\mu\text{m s}^{-1}$)
E	Electric field strength (volts cm^{-1})
CCDs	Charge-coupled devices
A_λ	Absorbance
I	Intensity
l	Optical path length
c	Concentration
T_λ	Transmittance
R	Radius of particles
X	Distance between the rotation axis and a specific position in the centrifuge tube
g	Gravity
d	Diameter

✉ Liu Yang
windy4ever@163.com

¹ Key Laboratory of Energy Thermal Conversion and Control of Ministry of Education, School of Energy and Environment, Southeast University, Nanjing 210096, China

² College of Materials Science and Engineering, Nanjing Forestry University, Nanjing 210037, Jiangsu, China

³ College of Materials and Chemistry and Chemical Engineering, Chengdu University of Technology, Chengdu 610059, China

D	Translational diffusion coefficient
R_H	Dynamic radius of the fluid
K_B	Boltzmann constant
T	Temperature

Greeks

ζ	Zeta potential
ϵ	Permittivity
η	Viscosity
α	Absorptivity
ω	Angular velocity of the centrifuge
ρ	Density

Subscripts

T	Total potential energy
VdW	Van der Waals
EP	Repulsive potential
R	Relative
O	Vacuum
i	Incident
t	Terminal
p	Particle
b	Base fluid

Introduction

Background

The global demand for energy coming from the refining and processing of natural crude oil and combustion of fossil fuels including coal and natural gas, is increasing rapidly due to the huge population of the world and the speedy development of industry [1]. However, these energy sources are not renewable because fossil fuels and natural crude oil can only be obtained through geological changes of more than 10,000 years. According to the speed of human energy consumption today, the reserve of fossil energy discovered on earth will soon be declared exhausted. In addition to the energy crisis, on the other hand, the exploitation and utilization of fossil energy will cause serious pollution to the environment, such as industrial wastewater, soil acidification, the greenhouse effect and other issues [2, 3]. Therefore, the search for clean and environmental-friendly renewable energy has become a global focal point in addressing the problem of scant sources and the damage to the environment. Solar energy has great potential because it is inexhaustible and non-polluting to the environment [4]. The solar radiation hits the earth with huge energy, which reaches the surface of the earth in one hour is more than the global energy needed in a year [5, 6]. Utilizing the solar energy of earth efficiently will help reduce carbon emissions and provide a possible way to tackle the energy crisis.

Water is the most widely used heat transfer medium in solar collectors because water is cheap and easily available. However, the further development of solar collectors is limited due to the scant absorption of water to solar radiation and the not good thermal conductivity. It is reported that just 13% of the energy reaching the earth from the sun can be absorbed [7]. Upgrading the efficiency of solar collectors by improving the structure of solar collectors is one of the methods, but it has not been widely studied because this method is economically expensive and has little effect, so many researchers have to focus on finding other types of heat transfer medium which have good thermal physical properties. The fluids that contain nanoparticles, typically between 1 and 100 nm in size, are called NFs. The NFs are widely used in heat exchanger [8], cooling [9], solar energy-collecting [10], desalination [11] and so on. For heat exchanger with different geometries, such as H-shaped cavity with porous media [12], heat pipe [13], double-layered microchannel [14], wavy microchannel [15], using NFs can markedly enhance the heat transfer efficiency of heat sink. For example, Tariq et al. found that, compared with water, the TiO_2 - H_2O NFs can effectively reduce the bottom temperature when they studied the heat dissipation of microchannel [16].

This is largely attributable to the enhanced thermal conductivity of the base fluid by the nanoparticles. In 1995, Choi et al. [17] found that the incorporation of small-size particles in the fluid can significantly enhance the thermal conductivity of fluids, from then on, NFs received widespread attention. The addition of nanoparticles will change the thermos-physical properties of the fluid. Some experimental results have shown that after adding trace amounts (ppm) of metals, oxides, carbon nanotubes (CNTs), graphene, Au/TiN, TiN and other nanoparticles to the fluids which including water, oil, and ethylene glycol (EG), can significantly improve the efficiency of heat collection. For example, the volumetric solar receivers using graphene-NFs with a concentration of 0.0005–0.001 mass% can improve the efficiency of heat collection by up to 70% [18]; Chen et al. found that the transmission of 0.03 mass% SiC-NFs over the entire wavelength range rate can be reduced to zero [19]. Such NFs, which are used for solar heat collection due to their excellent photo-thermal properties, are called solar NFs [20]. Figure 1 lists several common NFs that can be used for collecting solar energy. Besides, for direct absorption volume collectors, solar NFs can be used as both the carrier for the absorptions of solar radiation and the working medium for heat transfer, while for surface solar absorbers, it can just enhance the heat transfer.

There are two main ways to harness solar energy. One is that photovoltaic cells convert radiation into direct current under the exposure of sunlight, while the other one is that the solar collectors convert solar radiation into heat

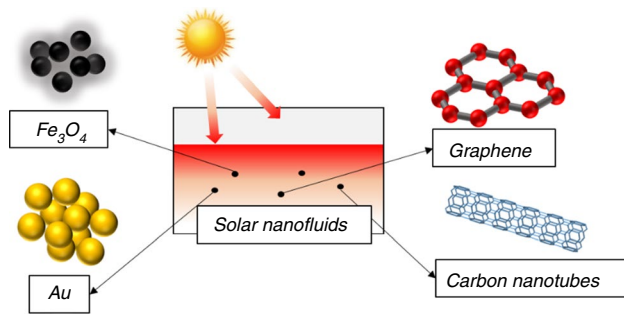


Fig. 1 Schematic diagram of some types of solar NFs

energy through the heat transfer medium. In photovoltaic systems, NFs can effectively reduce the increase in temperature of photovoltaic cells caused by continuous heat absorption, thereby improving the efficiency of photovoltaic systems [21–23]. Hence, photovoltaic systems can convert solar energy into electricity and thermal energy simultaneously, which is called photovoltaic thermal (PV/T) system [24]. Besides, the NFs can be an optical filter to absorb solar energy that the PV system cannot convert to achieve cooling [25]. Solar collectors involve the forms of the flat plate, parabolic trough, vacuum tube and direct absorption volume and so on [26]. The heat transfer medium plays an important role to determine the photo-thermal conversion efficiency and transmission efficiency of the system [27]. Except for ameliorating the structure of heat collectors, many researches [28, 29] have adopted NFs as work fluid. In the parabolic solar device with a wavy absorber pipe, the use of CuO-oil NFs can greatly improve the heat transfer coefficient [30]. Some scholars also said that adding turbulators and using hybrid nanomaterial containing CNTs and Al_2O_3 can increase the Nu by 75.22% [31].

With the aggravation of the energy crisis and environmental pollution, the literature on finding clean and renewable energy that can replace fossil energy, such as solar energy, is also increasing year by year. Experiments have verified that NFs can be used as a working medium in heat collectors. However, most of the review articles on NFs are focused on the summary of their physical properties, and there are few review articles on NFs that can absorb solar radiation. Therefore, this paper only focuses on solar nanofluids, which can efficiently absorb solar radiation, and summarizes its preparation mechanism and common problems in obtaining a stable state. More importantly, the experimental research and numerical simulations of solar NFs in solar heat collection are comprehensively compared and analyzed. This work provides theoretical support for finding stable and efficient solar nanofluids.

Aim of this review

Nanofluids have been widely used in various fields. Yang et al. [32, 33] summarized and analyzed the topics of those review papers on NFs in 2014–2016 and 2017–2019, and found that the contents of those research are mainly about the preparation and evaluation of NFs [34, 35], various physical properties [36] and forms of heat transfer and flow [37, 38], the application of heat exchange [39], refrigerated air conditioning [29, 40] and solar collectors [41, 42]. Most of the reviews focused on the summary or analysis of properties of NFs or different solar collectors with nanofluids, while the review on the preparation, stability and collecting efficiency of solar nanofluids is blank [20]. Therefore, it is necessary to implement a much-needed and detailed latest literature on the preparation, stability and solar thermal properties of solar NFs. In this paper, a critical analysis of techniques to prepare NFs is firstly made, and then the stability mechanism and influencing factors are elaborated in detail, and besides that, the evaluation techniques for the stability of solar NFs are reviewed. According to the latest research, some points on the photo-thermal properties of solar NFs are summarized and discussed. In the end, based on a large number of experimental and numerical research reviews, a series of problems to be handled about the utilization of solar NFs and the challenges faced in the commercialization process are pointed out and suggestions for further development and research of solar NFs in the future are proposed. The layout of the review paper is shown in Fig. 2 as follows.

The preparation of nanofluids

Long-term stability is one of the bottleneck issues in the commercialization of NFs. Under the influence of gravity and Van der Waals forces, nanoparticles tend to form clusters and settle in the base fluid. The ways for preparing stable NFs have become essential. In this section, the preparation methods of NFs which mainly consists of a one-step method and a two-step method will be comprehensively analyzed, and other preparation methods will be briefly introduced.

The one-step method

The method of simultaneously synthesizing nanoparticles and dispersing them in a base fluid using physical methods or liquid chemical techniques is called the one-step method. A summary of techniques of the one-step method for the preparation of NFs is shown in Fig. 3. The physical method includes vapor deposition, laser ablation and submerged arc, which is often used to prepare metal and metal oxide nanoparticles. EG-based ZnO NFs were successfully

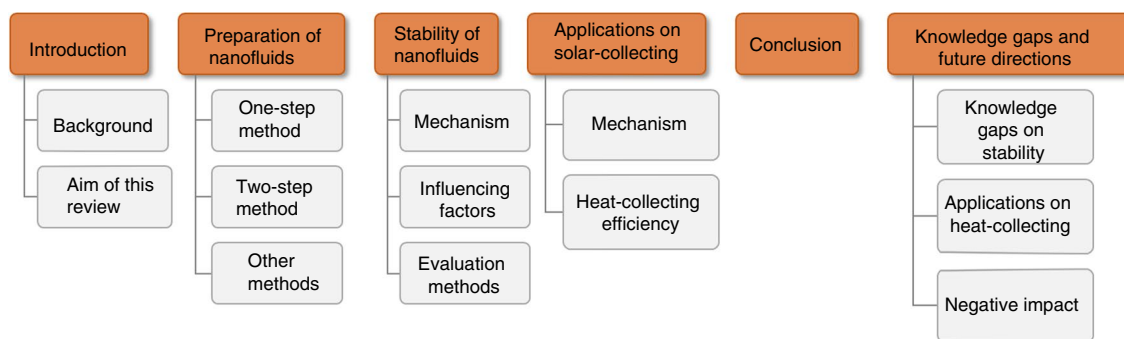


Fig. 2 The overall layout of this review paper

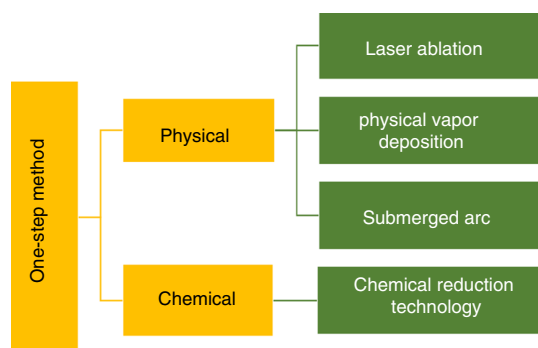


Fig. 3 The specific technologies for preparing NFs by one-step method

prepared by one of the physical methods called the pulsed-wire evaporation (PWE) technology [43], which uses 26kv pulsed high voltage to superheat and evaporate pure zinc thin wires into plasma. For Cu-water NFs, electro-explosive wire (EEW) technology can be used to synthesize copper

nanoparticles with a diameter ranging from 30 to 50 nm, which can stay stable for 72 h [44]. In addition, chemical methods such as chemical reduction are also commonly used in the one-step method for the preparation of NFs. For example, Zhu et al. [45] used chemical reduction technology to reduce $\text{CuSO}_4 \cdot 5\text{H}_2\text{O}$ by using $\text{NaH}_2\text{PO}_2 \cdot \text{H}_2\text{O}$ and EG under microwave irradiation, then on that basis, a stable Cu-EG nanofluid was prepared. The following year, Zhu et al. [46] prepared Fe_3O_4 nanofluids with different concentrations by co-precipitation method. The commonly used preparation method of silica NFs is the sol-gel method, and many researchers have successfully synthesized silica NFs by this method [44, 47]. Table 1 lists the relevant literature using the one-step method to prepare NFs. Based on a comprehensive analysis of the latest reports, the evaluations on this method are listed next:

The advantages of the one-step method for the preparation of NFs are as follows:

Table 1 A review of the one-step method to output the solar NFs

Type	Researcher	Base fluid	Shape & size	Concentration	Technology
Cu	Khoshvaght-Aliabadi [50]	Water	Spherical, $d = 30\text{--}50$ nm	0.1mass%, 0.3mass%	EEW technology
	Zhu [45]	EG	Spherical, $d < 20$ nm		Chemical reduction
	Kumar [51]	EG	740 nm	0.1 M	Chemical reduction
Fe_3O_4	Zhu [46]	Water	Spherical, $d = 10$ nm	0–1%	Co-precipitation
ZnO	Lee[43]	EG	Spherical, rectangle, $d < 100$ nm	0.5, 1.0, 2.0, 3.0, 4.0, 5.5 vol.%	Pulse line evaporation, physical method
Ag	Salehi[52]	Distilled water (DW)	Spherical, $d = 5$ nm	0–1000 ppm	Chemical reduction
	Ashok[53]	Ethanol	Spherical, 30 nm, 60 nm		Chemical reduction assisted by microwave
	Bönnemann[54]		9.5 nm	0.3, 0.011 vol.%	Chemical reduction
C	Teng[55]	DW	500–4500	0–0.4 mass%	Water-assisted synthesis
CuO	Lo[56]	DW	Spherical, 49.1 nm		Submerged arc
Al_2O_3	Hung[57]	Water	10–30 nm	0.5, 1, 3 mass%	

- The prepared NFs have better stability, and the time of aggregation and sedimentation of the particles in the base liquid is greatly extended.
- Synthesize types of NFs directly can avoid the occurrence of agglomeration during the process of drying, transport, and dispersion of nanoparticles in the two-step method, guaranteeing the good stability of NFs.

- The size of the nanoparticles synthesized by the one-step method is controllable and small, and the shape and size of nanoparticles can be controlled by varying pH, temperature, and concentration of individual components [48].
- Oxidation of nanoparticles can be avoided while preparing pure metal NFs.

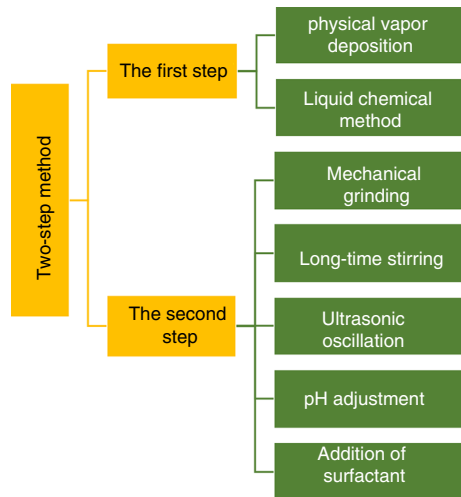


Fig. 4 The specific technologies for preparing NFs by two-step method

However, there are main reasons why this technology cannot be industrialized, which are shown as follows:

- The one-step method for preparation is complex and the cost of equipment is high, so it cannot be produced in large quantities, which is the major reason why the one-step method cannot be used widely.
- The one-step method is only suitable for low vapor pressure fluids, causing a small range of applications of this method [48].
- Residues produced during preparation can have a negative effect on the NFs [49].

The two-step method

The two-step method refers to the process of synthesizing nanopowders firstly and dispersing them into the base fluid secondly to prepare NFs. The techniques for the yielding of NFs are summarized in Fig. 4, and Table 2 summarizes the

Table 2 A review of the two-step method to output solar NFs

Type	References	Dispersants/surfactants	pH	Other methods
Cu	[64]	Oleic acid		Ultrasonic vibration for 10 h
CNTs	[60]	N-hydroxysuccinimide		Magnetic stirring, Ultrasonic vibration
	[65]			
Al ₂ O ₃	[66]		Nitric acid treatment	Ultrasonic vibration
	[62]		4.9	Ultrasonic vibration for 4 h
	[67]		5.5	Ultrasonic vibration for 4 h
	[68]	Sodium dodecylbenzenesulfonate (SDBS)	HCl + NaOH	
	[69]	SDBS cetyltrimethylammonium bromide (CTAB)	HCl + NaOH	Ultrasonic vibration for 20 min
ZnO	[70]			Ultrasonic vibration for 4–100 h
Fe ₂ O ₃	[63]	Polyethylene glycol	11.1	Magnetic stirring for 1 h
	[71]	Nonylphenol ethoxylate	9.1(0.1 mass%) 9.6(0.3 mass%)	Ultrasonic vibration for 30 min
CuO	[58]			Magnetic stirring, Ultrasonic vibration
	[72]			Ultrasonic vibration for 30 min
Fe ₃ O ₄	[59]	Tetramethyl ammonium hydroxide		
TiO ₂	[73]		7.5 (0.2 vol.%) 7.1 (0.6 vol.%)	

literature on the preparation of different kinds of NFs using the two-step method. Several methods are used to synthesize nanopowders, which include chemical vapor deposition techniques and wet chemical methods. The wet chemical method is more suitable for the preparation of metal oxide NFs, the principle of which is to extract metal oxide nanoparticles from metal salts through chemical reactions. For example, CuO nanopowders are usually produced by this method using CuSO_4 as the precursor, and the high-temperature annealing process is used to purify the copper oxide nanoparticles during the preparation process [58]. Fe_3O_4 nanoparticles can be obtained from $\text{FeCl}_3 \cdot 6\text{H}_2\text{O}$ and $\text{FeCl}_2 \cdot 4\text{H}_2\text{O}$ under the action of ammonia water [59]. However, the vapor deposition method is mostly used to prevent oxidation of nanoparticles and multi-walled carbon nanotube powders. Liu et al. [60] used the catalytic chemical vapor deposition method to prepare the multi-walled carbon nanotube powder. In addition, different from the general gas-phase technology, Kathiravan et al. [61] used high-voltage direct current magnetron sputtering to prepare copper nanoparticles for the first time, with an average particle size of 10 nm.

It is less difficult to synthesize nanopowders compared with the one-step method, and the process of producing some kinds of nanopowders has been industrialized. Therefore, it can be convenient for many experiments to directly purchase nanopowders and then disperse them into basefluid. However, there is a problem that nanopowder is easy to agglomerate during the process of storage and dispersing. In order to keep it dispersed in the base liquid uniformly, these ways are adopted usually: 1. Grinding nanopowder mechanically; 2. Long-time stirring; 3. Ultrasonic treatment; 4. Adjusting pH value; 5. Adding surfactants. For the propose of stably suspending copper nanoparticles in the base liquid, Kathiravan et al. [61] vibrated the nanofluids in an ultrasonic bath for about 10 h, and finally obtained a uniform copper–water nanofluids; Similarly, to prepare dispersed evenly and stable CNT-ethylene glycol NFs, the method of magnetic stirring and ultrasound homogenize the nanofluids are utilized at the same time [60]. According to the experimental results of Qu et al. [62], the alumina nanoparticles remain stable for 72 h when the pH value was 4.9, and they succeeded in using electrostatic stabilization technology and ultrasonic vibration for 4 h to disperse the suspension uniformly. Besides, it is reported that Fe_2O_3 -water nanofluids have the best stability when $\text{pH} = 11.1$. Apart from this, at this pH value, adding 0.8 mass% polyethylene glycol can ensure the stable dispersion of Fe_2O_3 nanoparticles in DW for a week. During preparation, they were also magnetically stirred for about 1 h to ensure the uniformity of nanoparticles [63]. Abareshi

et al. [59] dispersed the prepared Fe_3O_4 nanoparticles in DW, and added a dispersant to overcome the effects of magnetic and van der Waals forces and reduce the agglomeration of nanoparticles.

Based on the mature industrial technology, the two-step method is a widely used and simple way for preparing NFs. The advantages are as follows:

- It is more convenient for researchers to obtain nanopowder because the process of synthesizing nanopowder is relatively mature and large-scale production has been realized.
- The means to maintain good dispersion and stability of NFs during experiments, which refer to magnetic stirring, ultrasonic oscillation, adjustment of pH and adding dispersant, are simple and feasible.

But the disadvantages are also obvious:

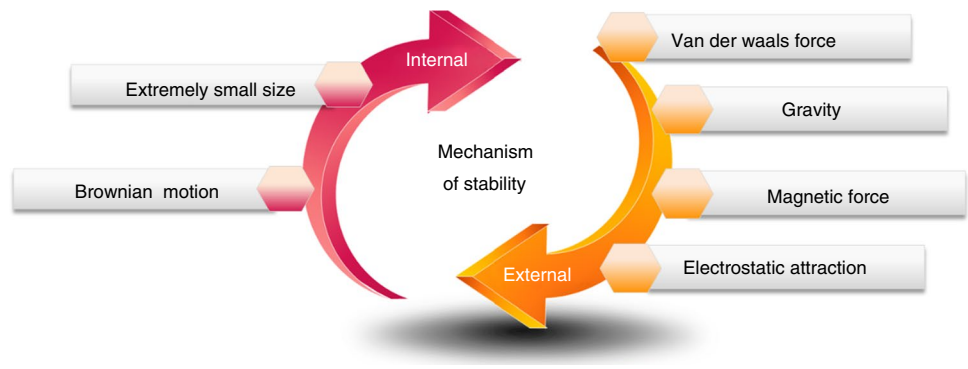
- Nanoparticles are prone to agglomerate during the process of storage, transportation and dispersion, so a range of means are needed. Nevertheless, the stability of NFs prepared by the two-step method is still inferior to that of the NFs prepared by the one-step method.
- Although metal particles can be prepared in inert gases, it is susceptible for metal nanoparticles to occur oxidation when dispersed.
- Compared with the one-step method, the two-step method cannot achieve precise control of the diameter of nanoparticles.

Other technologies

For some NFs which are in poor dispersion or already formed agglomerates, the method to obtain NFs with better dispersion by some special methods is the post-processing method. For example, the initial agglomeration of CB and Ag nanofluids was not effective by means of stirring, ultrasonic bath and breaker; however, the size of those two nanoparticles after high-pressure homogenizer treatment could get good results (45 nm and 35 nm) [74].

The method of changing the synthesis environment of nanoparticles from polar to non-polar (and vice versa) is the phase treatment method, which is suitable for the insolubility problem during the preparation of nanofluids [75]. Some mental nanoparticles, such as Ag, Au and Pt, could realize the transfer from the aqueous phase to the 1-butanol phase transfer [76]

Fig. 5 Schematic diagram about the mechanism of stability of NFs, which include internal reasons (small size and Brownian motion) and external reasons (Van der Waals force, gravity, magnetic force and electrostatic attraction)



The stability of nanofluids

Mechanism of stability

Since there is no chemical reaction between the nanoparticles and the base liquid, the instability of the NFs is manifested as agglomeration and sedimentation of the nanoparticles. Obviously, unstable solar NFs will no longer have excellent performance on heat collection, which is also the biggest obstacle to the industrialization of solar NFs. Figure 5 shows the factors affecting the stability of NFs. There are many reasons for the instability of solar NFs, which are summarized into two categories in this paper: internal effects and external forces. The internal reason is reflected in the characteristics of the nanoparticles themselves. Due to their extremely small size, nanoparticles have the extremely large specific surface area and specific surface energy, which are thermodynamically unstable [77]. Because of the existence of Brownian motion, small-sized nanoparticles move faster and have a greater chance of colliding. Particle-to-particle collisions may produce adhesion effects, resulting in nanoparticle clustering [78]. External forces mainly include Van der Waals force, gravity, magnetic force, electrostatic attraction, etc. Under the action of these external forces, nanoparticles are very easy to aggregate and cause inevitable precipitation under the action of gravity. The DLVO theory is commonly used to explain the mechanism of dispersion of suspensions [79]. This theory has four assumptions: (1) the nanoparticles are uniformly dispersed; (2) only the Van der Waals and electrostatic forces are considered; (3) the effects of buoyancy and gravity are omitted; (4) The ion distribution in the base fluid is only affected by three factors: Brownian motion, electrostatic force, and entropy [80]. The theoretical expression of DLVO is Eq. (1):

$$F_T = F_{VdW} + F_{EP} \tag{1}$$

where F_T is the total potential energy, which is the sum of the attraction potential (F_{VdW}) and the repulsive potential (F_{EP}) between particles. The attractive potential between particles is from the Van der Waals force, and the repulsive potential depends on the electrostatic repulsion. Obviously, if the Van der Waals force between the particles is stronger than the electrostatic repulsion, then the total potential energy appears as an attractive force, and the nanoparticles are prone to aggregate to form clusters, resulting in a decrease in the stability of the NFs. The expressions of the two forces are related to elements which are size, shape and concentration of nanoparticles.

Influencing factors of stability

Many factors affect the stability of NFs, including the dielectric constant of base fluid, pH value, surfactant, zeta potential, size, shape and concentration of nanoparticles. These factors all affect the stability of NFs by directly or indirectly influencing the attraction or repulsion between particles, which are displayed in Fig. 6. And the details will be explained next.

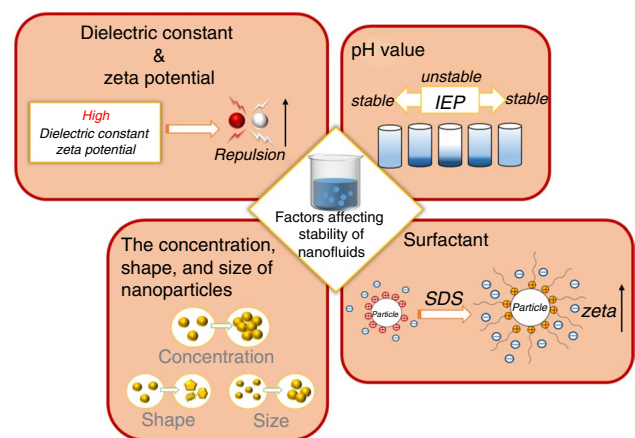


Fig. 6 Schematic diagram of factors affecting the stability of NFs

Dielectric constant of base fluid & zeta potential

The dielectric constant of the base fluid is one of essential to impact the stability of the NFs, and a high dielectric constant means a higher repulsive potential, which is beneficial to the stability of the nanofluids. It is discovered that the highest dielectric constant is water because the fact that the dielectric constant of common base fluids, for example, the acetone is 21.01, the ethanol and EG are 24.6, while water is 78.5, so pure water is the most common base fluid in the preparation of NFs [81]. The higher the zeta potential value of the NFs, the greater the repulsive potential between particles. A more detailed explanation of the zeta potential will be carried out in the next section, so it will not be repeated.

The value of pH

Changing the pH value of the liquid is actually changing the charge density on the particle surface, and enhancing the stability by strengthening the electrostatic repulsion. The isoelectric point (IEP) refers to the zero zeta potential of the fluid, at which point the repulsive force and the attractive force are in equilibrium, and the NFs is in an unstable state. If the pH value is controlled at the pH value far from the isoelectric point of the suspension, the suspension is stable. Relevant experiments have confirmed this phenomenon: 11 samples with a pH value of 2~12 were prepared in an experiment and the pH value of TiO_2 -water nanofluids with a concentration of 0.25 vol.% at IEP is 6.5. The samples with pH = 6 firstly appeared in precipitation. After two weeks, the samples with a pH of 4 to 8 were no longer turbid and became clear liquids. After 30 days, only the samples with a pH of 12 maintained good stability [82]. However, the optimal pH values for maintaining the stability of different NFs are different. For example, Al_2O_3 -water NFs reach the

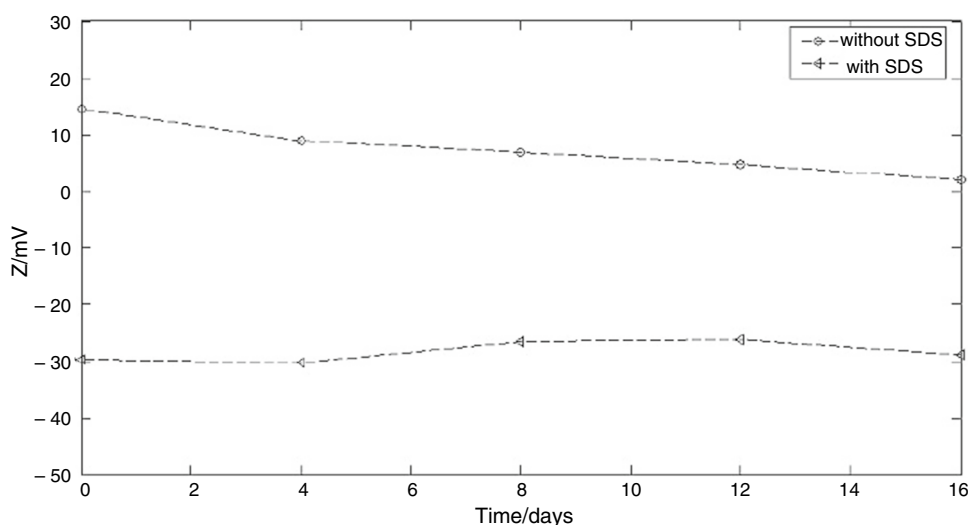
maximum zeta potential at pH = 8, which is -40.1 mV; Cu-water NFs reach the maximum zeta potential at pH = 9.5, which is -43.8 mV [83].

Surfactant

Adding surfactants to the fluid can effectively improve the stability of NFs. The surfactant is amphiphilic due to the molecular structure which is composed of two ends of a hydrophilic group and a hydrophobic group, respectively. Appropriate amount of surfactants can affect the surface properties of NFs, such as anionic surfactants, the positively charged head is adsorbed by the nanoparticles, and the negatively charged tail is freed in the electric double layer of nanoparticles, causing an increasing of (negative) zeta potential.

Figure 7 shows the zeta potential of the Al_2O_3 -water nanofluids with and without sodium dodecylsulfate (SDS). It can be seen that the zeta potential of the nanofluids without SDS is +15 mV and gradually decreases with time, indicating that this nanofluid is unstable. After adding SDS, the zeta potential of the nanofluids was maintained at about -30 mV for 16 days, which shows that the addition of SDS greatly improved the stability of the nanofluids [84]. However, there are many types of surfactants, and how to choose the most suitable surfactant is also a key issue. MWCNT has poor stability due to its unique large aspect ratio structure, so surfactants are often added when preparing MWCNT-NFs. Surfactants which are commonly used include SDBS, CTAB, SDS, Gum Arabic (GA), etc. Choi et al. [85] experimentally studied the effect of four surfactants on the stability of MWCNT NFs. By comparison, SDBS and Triton X-100 (TX-100) NFs gave the best performance, followed by CTAB NFs, and SDS NFs dropped most in suspension stability within 1 month. And they also

Fig. 7 The contrast about the zeta potential of 0.01 vol.% Al_2O_3 -water with and without SDS in 16 days. (Reprinted from ref [84], with permission from Elsevier)



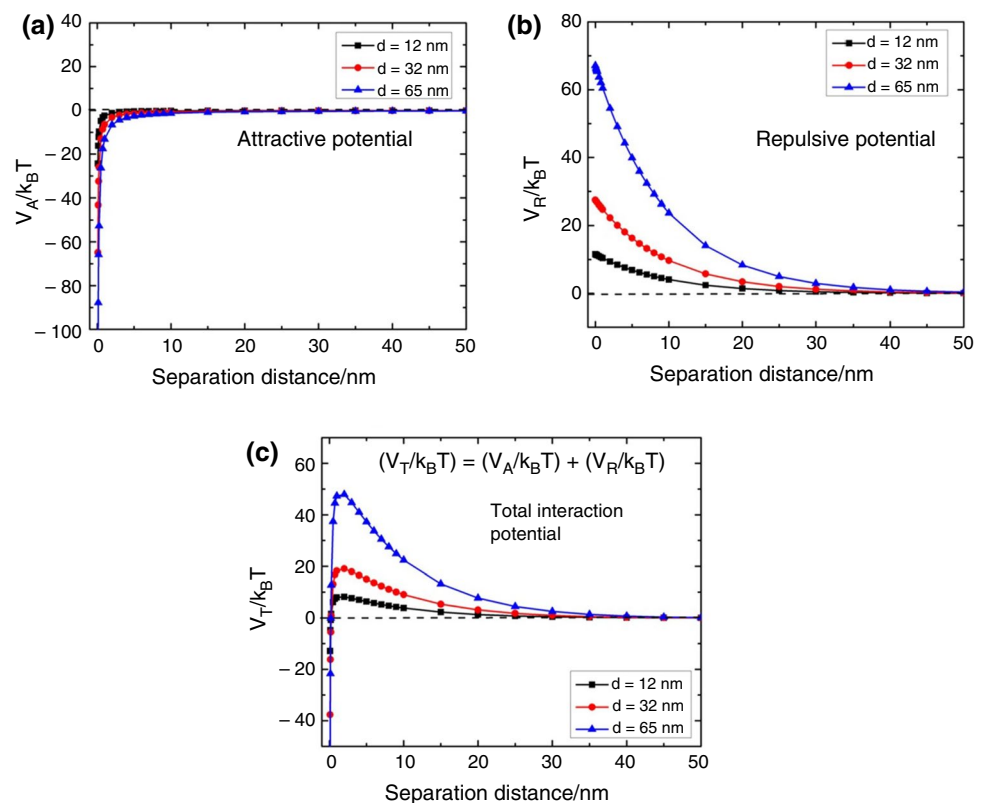
concluded that temperature can affect the effect of surfactant to a certain extent.

The concentration, shape, and size of nanoparticles

The properties of nanoparticles such as size, shape and concentration can also impact the time of nanofluids to maintain stable. Both Van der Waals and electrostatic repulsion will change with the variety of sizes and shapes of nanoparticles. The classical DLVO theory is applicable to spherical nanoparticles. While the nanoparticles are no longer spherical, the expression of electrostatic repulsion will be more complicated. Some scholars have summarized the electrostatic repulsive interaction potential and Van der Waals attractive interaction potential under different boundary conditions with various shapes [81]. Compared with spherical particles, nanoparticles with high aspect ratios (such as MWCNTs) are more likely to form clusters, and the action potential in the parallel direction is stronger than that in the vertical direction. For asymmetric nanoparticles, Van der Waals attraction is more dominant than electrostatic repulsion, and its aggregation may be greater [86]. Kim et al. [87] measured the stability of water-based boehmite alumina NFs of different shapes (brick, plate, and leaf). Under the same volume fraction, pH value and temperature conditions, the shape of the particles suspended in the base liquid changed from leaf

to plate and finally to brick, which indicates that the leaf-like nanoparticles are easier to aggregate, and the aggregated nanoparticles will settle rapidly. The total potential energy of nanoparticles with different particle sizes is different. The decrease in particle size causes an increase in the number of atoms on the surface of the particle, and thus the attractive potential between particles increases. Many literature reported that the gathered tendency of small-sized nanoparticles is stronger. As shown in Fig. 8, with the increase in hematite ($\alpha\text{-Fe}_2\text{O}_3$) particle size, the repulsive potential between particles increases. Obviously, the change in attractiveness is weak but the overall trend is decreasing. The Van der Waals force increases as the distance between particles decreases, so when the concentration of nanoparticles in the fluid increases, the attractive potential between particles increases correspondingly, and the increase in particle concentration will increase the size of particle clusters. Therefore, the phenomenon of agglomeration and sedimentation is more likely to occur in the nanofluids with high concentration. The Cu–Zn–Al LDH nanofluids was reported to be stable at 40 ppm, but precipitation was observed at 240 ppm, and the aggregated size increased with the addition of particle concentration [88].

Fig. 8 The attractive potential, the repulsive potential and the total interaction potential of different diameters of nanoparticle ($\alpha\text{-Fe}_2\text{O}_3$). (Reprinted from ref [81], with permission from Elsevier)



Evaluation methods of stability

Measurement of zeta potential

Zeta potential is a common method for measuring the tendency of NFs to form aggregates. When the nanoparticles are dispersed in the fluid, a fixed layer (Stern layer) and a dispersion medium layer (diffusion layer) will be formed on the surface of the particles. The potential difference between the two layers is the zeta potential (ζ). The Stern layer is closer to the surface of the nanoparticle with ions on it, which are opposite of the surface; while outside the stern layer is the diffusion layer, which includes both the positive and negative ions. The zeta potential can be got by the following Equation [80]:

$$\mu_e = \frac{V}{E} \quad (2)$$

where V means the velocity of nanoparticles ($\mu\text{m s}^{-1}$) and E means electric field strength (volts/cm). ζ can be obtained by Henry equation:

$$\mu_e = \frac{2\varepsilon_r\varepsilon_0\zeta f(ka)}{3\eta} \quad (3)$$

where ε_r is relative permittivity, ε_0 is vacuum permittivity, $f(ka)$ is Henry function, and η is the viscosity at the experimental temperature.

The larger the zeta potential value, the stronger the electrostatic repulsion between nanoparticles, the weaker the assembly of nanoparticles, and the better the stability of the nanofluids. On the contrary, the smaller the value of ζ , the worse the stability of the nanofluids. In general, NFs are considered to be electrostatically stable when the zeta potential is $> \pm 30$ mV, and NFs are considered to remain stable for a long time when the zeta potential is $> \pm 60$ mV [80]. If the

zeta potential is ± 15 mV, some scholars have indicated that when the zeta potential is $0 \sim \pm 5$ mV [48], the nanofluids are prone to occur agglomeration. Studies have shown that the value of zeta potential can be increased by changing the pH of the fluid, adding surfactants or functionalizing nanoparticles. When the pH value changes from the isoelectric point ($\zeta = 0$), the electrostatic charge on the surface of the nanoparticles will increase, and the repulsion between the particles will become larger, thereby obtaining a stable suspension [89]. The Fe_3O_4 -Water NFs with a mass concentration of 0.1–0.3 mass%, when the pH value is adjusted between 9 and 10, the measured zeta potential is -32 mV, which can remain stable for 504 h [71]. The Al_2O_3 -Water nanofluids had the best zeta potential value when 0.064 mass% SDBS was added [69]. Sarsam et al. [90] also indicated that when the concentration of GNPs and SDBS was 1:1, the GNP-water nanofluids had the best stability, and the zeta potential value was -45.6 mV. Table 3 lists the relevant literature on the measurement of solar nanofluids stability by the zeta potential method.

However, zeta potential measurement has limitations on the viscosity and concentration of NFs [91], and the zeta value is only a predictor of particle agglomerated tendency and should therefore not be considered as a final measure of nanofluids stability [80].

Measurement of spectral absorbance and transmittance

When ultraviolet or visible light passes through the NFs, it will be absorbed to different degrees, so the stability of the NFs can be judged by measuring the change of the absorbance or transmittance of the NFs with time. The unstable NFs will form deposition at the bottom, and the decrease in the concentration of nanoparticles in the upper layer will lead to a decrease in the absorption of light. Therefore, if the measured absorbance decreases with time or the

Table 3 A review of the stability of solar NFs measured by zeta potential

Nanofluids	pH	Dispersant	Zeta potential
Cu-water [92]	–	SDBS	-43.8 mV
Fe_3O_4 -Water [71]	pH=9.1, 9.6, 10.1 (0.1–0.3 mass%)	Nonylphenol Ethoxylate	-32 mV
CuO-DI Water [93]	pH=10.2	SDS	-11.94 mV
ZnFe_2O_4 -water [94]	–	CTAB	30–42 mV
Al_2O_3 -Water [94]	–	CTAB	45 mV
Al_2O_3 -Water [69]	pH=8.6	SDBS, CTAB	≥ 30 mV
GNP-water [90]	pH=7.6 (SDBS) pH=7.42 (SDS) pH=4.78 (CTAB) (after ultrasonic vibration for 1 h)	SDBS, SDS, CTAB	-18.5 mV (SDS) -45.6 mV (SDBS) 26.6 mV (CTAB)
GNP-water [95]	–	Pluronic P-123	-31.9 mV
MWCNT-water, [96]	pH=7	GA, PVP, SDS	-58.0 mV (SDS), -47.5 mV (GA), -45.6 mV (PVP) (When the ratio of CNT to dispersant is 1:1)
Au-water, [97]	pH=4.0 \pm 0.37	–	-32.1 ± 0.95 mV (0.018 vol.%)

transmittance increases with time, it means NFs are unstable. Usually, this method is suitable for nanoparticles with absorption peaks between 190 and 1100 nm [98], but not for dark-colored NFs such as CNTs and high-concentration NFs. The equipment that provides the light source can be the He-Ni laser with a wavelength of 632 nm, and ultraviolet spectrophotometers and charge-coupled devices (CCDs) can capture images at specific wavelengths to complete the measurement of absorbance and transmittance [48]. The measurement principle of absorbance (A_λ) is as follows:

$$A_\lambda = \log(I_i/I) = \alpha \times l \times c \tag{4}$$

where I , I_i , α , l and c represent the intensity, intensity of the incident laser, absorptivity, optical path length, and particle concentration of the laser beam passing through the NFs, respectively. It is not difficult to see from formula (4) that the absorbance is proportional to the particle concentration. When the NFs is precipitated, the concentration of the supernatant decreases. The relationship between transmittance and absorbance (A_λ) is as follows:

$$T_\lambda = I/I_i \tag{5}$$

Figure 9 shows the absorption spectra of the Ultraviolet–visible spectroscopy of different kinds of NFs ((a) 1.0 mass% γ - Al_2O_3 , (b) 0.1 mass% α - Al_2O_3 , and (c) 0.01 mass% TiO_2 NFs) [99]. The absorption rate of the three NFs showed a steady downward trend with time, and the stability of γ - Al_2O_3 with high concentration was much stronger than that of α - Al_2O_3 NFs with low concentration. Interestingly,

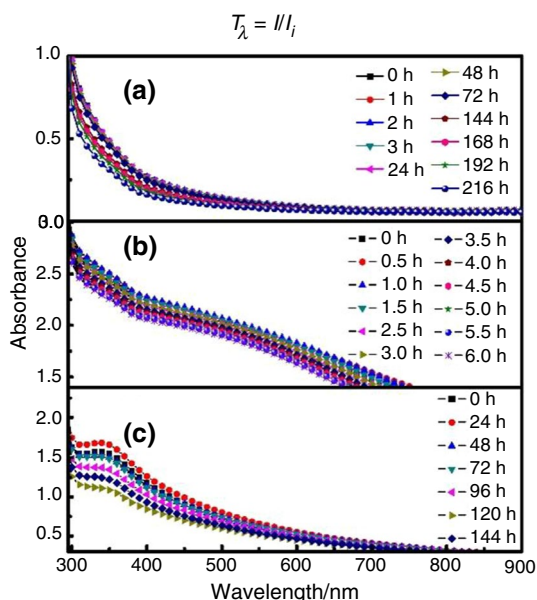


Fig. 9 The absorbance of different NFs with the change of time. (Reprinted from ref [99], with permission from Elsevier)

the stability of TiO_2 NFs with a concentration of only 0.01 mass% is not much different from that of γ - Al_2O_3 NFs with a concentration of 1.0 mass%.

Sedimentation and centrifugation

Nanoparticles will settle downward under the action of gravity, and agglomeration is likely to occur in suspensions with poor stability, which accelerates the precipitation of particles. The method that the precipitation of the NFs was observed by photographing technology is called the sedimentation method. The longer the precipitation time of the suspensions, the better the stability of the NFs. Some researchers have also judged the stability by observing the change of the precipitation height with time. The settling velocity could be got by the Stokes law which works for spherical particles:

$$V_t = \frac{2r^2(\rho_p - \rho_b)g}{9\eta} \tag{6}$$

where V_t refers to the terminal velocity, r is the radius of particles, ρ_p is the density of the particle, and ρ_b , g , and η means density, gravity and dynamic viscosity of the base fluid, respectively. Considering that the sedimentation takes a long time, the centrifugation is proposed to replace the sedimentation. The sedimentation of the fluid is accelerated by centrifugal force which is stronger than gravity. Replacing the gravity by centrifugal force in Eq. (5), we can get:

$$V_t = \frac{d_p^2(\rho_p - \rho_b)\omega^2 X}{18\eta} \tag{7}$$

where d_p is the diameter of the nanoparticle, ω is the angular velocity of the centrifuge, and X is the distance between the rotation axis and a specific position in the centrifuge tube. It can be seen from Eqs. (5) and (6) that the smaller the size of the nanoparticles, the higher the viscosity of the base fluid, the greater the relative density difference between the base fluid and the nanoparticles, and the lower the gravitational sedimentation velocity. But the size of nanoparticles cannot be as small as possible. Small-sized NFs have higher surface energy and are easy to form agglomerates, which is not conducive to the stability of NFs. Figure 10 shows the change of Al_2O_3 nanofluids with time [100]. It can be clearly seen from the figure that the transparency of the nanofluids becomes higher and higher with the passage of time and a white precipitate appears under the test tube. Although the sedimentation is simple to operate and does not require complicated equipment, its significant disadvantage is that it takes a long time, and usually observation for a period ranging from 1 to 30 days.

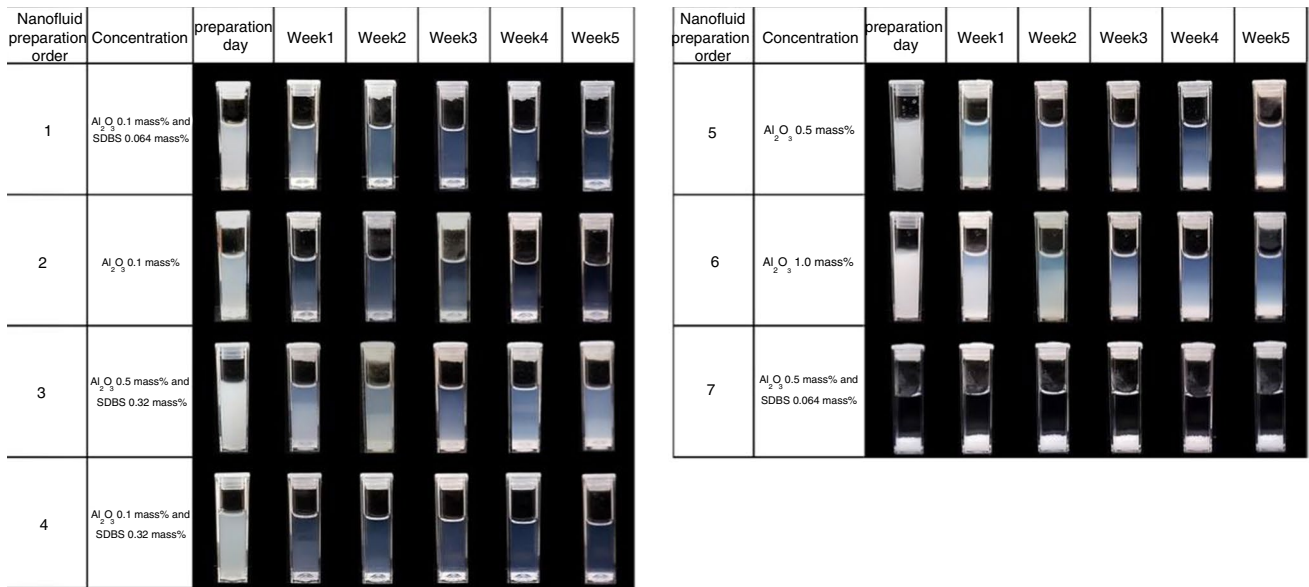
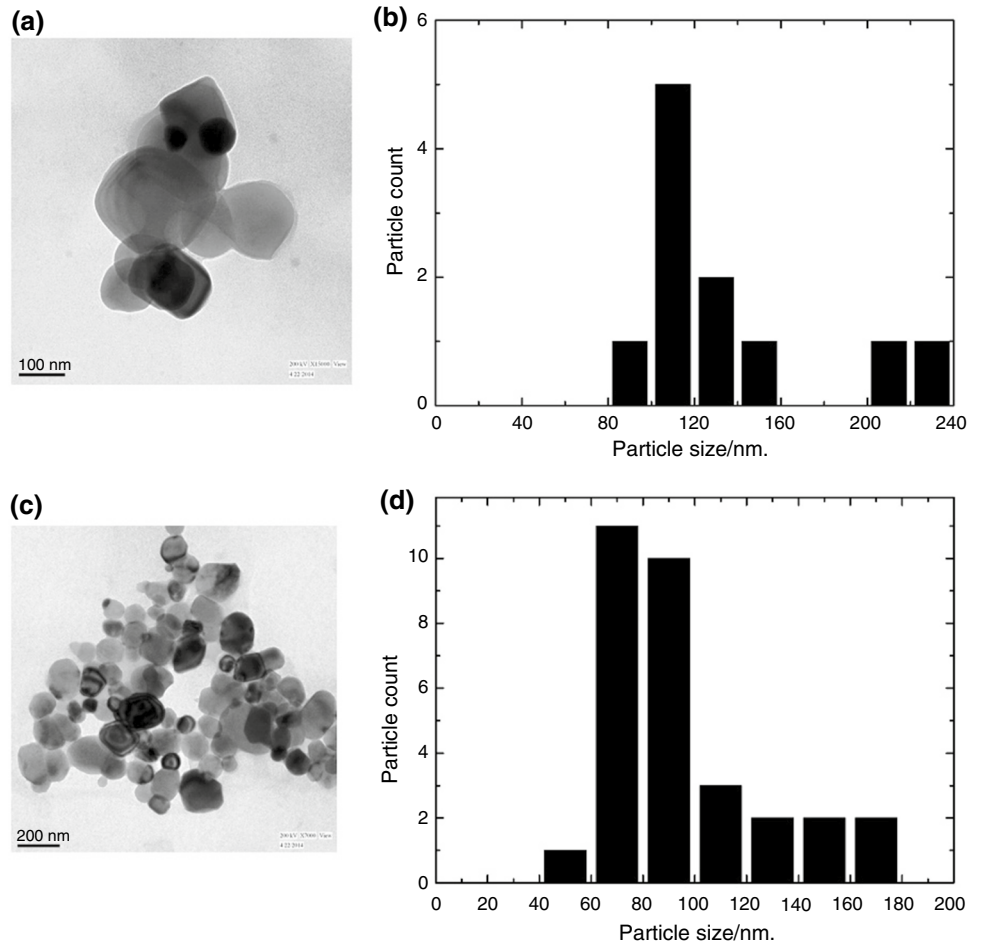


Fig. 10 Visual inspection of seven selected NFs. (Reprinted from ref [100], with permission from Elsevier)

Fig. 11 TEM images and histogram plot of TiO₂ with and without treatment. **a, b** Without treatment. **c, d** After treatment. (Reprinted from ref [101], with permission from Elsevier)



Transmission electron microscope (TEM)

Transmission electron microscopy can provide two-dimensional images of nanoparticles on the nanometer scale, which can be used to observe the agglomeration phenomenon of NFs, and is also a common method for measuring the diameter of nanoparticles. The operation steps are generally as follows: first, a small amount of nano-powder is attached to the carbon substrate. After sweeping away the excess nano-powder, the sample should be dried under a mercury lamp. Finally, the sample is scanned using a transmission electron microscope. All pre-scan steps are essential, if the sample is still wet, it will not be able to adhere to the carbon substrate. During the drying process, NFs of different morphologies are very likely to agglomerate, which is an unavoidable disadvantage of electron microscopy measurements. Figure 11 shows the TEM image of TiO₂ nanoparticles along with the particle size histogram [101]. It can be clearly observed that the TiO₂ nanoparticles have various shapes such as spherical, square and polygonal through TEM pictures. The histograms (b) and (d) can be obtained by counting the number of particles with different particle sizes in the SEM images.

Dynamic light scattering (DLS)

TEM technology is used to accurately measure the diameter of nanoparticles, and DLS can give the number of nanoparticles of different sizes. The measurement principle is to determine the stability of NFs by measuring the variety in size of suspended nanoparticles through a long time. Nanoparticles suspended in the fluid move caused by Brownian motion, leading to the oscillation of intensity of the scattered light which illuminates on nanoparticles. The fluctuation data of light intensity can be monitored and recorded by photon detectors. In unstable NFs, larger-sized aggregates will settle at the bottom of the container under gravity, resulting in

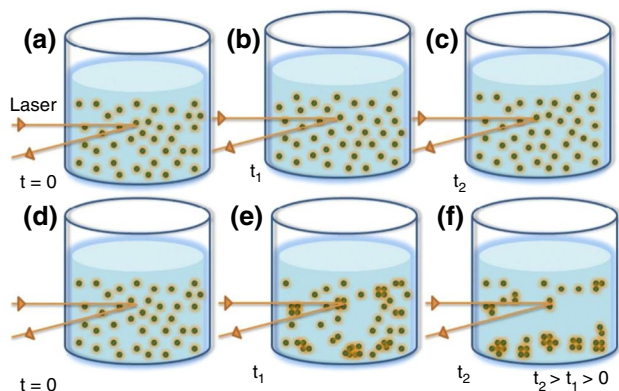


Fig. 12 The schematic diagram of scattering of laser light through NFs with different stabilities over a period of time. (Reprinted from ref [99], with permission from Elsevier)

reduced interaction between the nanoparticles and the laser in the supernatant. Figure 12 shows the schematic diagram of [99] scattering of laser light through NFs with different stabilities over a period of time. The principle of light scattering explains the relationship between the intensity of scattered light and the diffusion coefficient, which can be used to determine the size of nanoparticles in colloids using the Stokes–Einstein equation for the diffusion coefficient, as follows [102]:

$$R_H = \frac{K_B T}{6\pi\eta D} \quad (8)$$

where R_H is the dynamic radius of the fluid, K_B is the Boltzmann constant, T is the absolute temperature, η is the viscosity, and D is the translational diffusion coefficient. NFs with poor stability are agglomerated due to electrostatic interaction or other reasons, so the nanoparticle diameter measured is larger. That is, if the measured size of nanoparticles increases with time, it means that the NFs do not have good stability. However, this method is not suitable for high concentrations of NFs or when nanoparticles of various sizes are suspended in the base fluid, because DLS techniques give inconsistent size distributions. DLS technology can be combined with TEM technology to obtain precise nanoparticle size.

Figure 13 shows the distribution of particle size of Al₂O₃ NFs with the mass concentration of 1 mass% and the graph of the mean hydrodynamic diameter as a function of time,

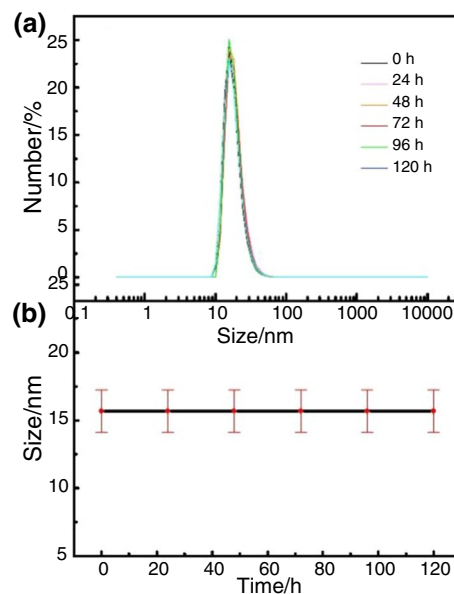


Fig. 13 The distribution of particle size of Al₂O₃ NFs with the mass concentration of 1 mass% **a** and the graph of the mean hydrodynamic diameter as a function of time **b**. (Reprinted from ref [99], with permission from Elsevier)

both were obtained by the DLS technique [99]. The distribution of particle size of the Al_2O_3 NFs remained unchanged during the observation period of 5 consecutive days, indicating that the NFs were stable. However, when the concentration decreased, it was observed that the peak of the distribution of particle size shifted significantly to the left when the mass concentration of Al_2O_3 NFs was 0.1 mass%, and the average horizontal dynamic diameter decreased from the initial 255 nm to 38 nm (after 5 h) showed poor stability.

Thermo-gravimetric analysis (TGA) of nanofluids

Unlike conventional stability measurement methods, thermogravimetric analysis aims to determine the thermal stability of NFs. A small amount of the sample is heated in a heat-resistant container (usually a heat-resistant ceramic crucible), and a very sensitive balance is set at the bottom to measure the mass of the sample. When the exact mass percentages of surfactant and nanoparticles in the fluid are known, thermal stability analysis of NFs can be performed in conjunction with the balance mass data. Studies have shown that the addition of carbon nanotubes can increase the thermal stability of heat transfer oil. The peak temperature of the mass loss changes of the heat transfer oil appeared at 388 °C. With the increase in the concentration of carbon nanotubes, the peak temperature of the mass loss change of the fluid gradually moved back. The largest change in mass loss of 1mass% carbon nanotube-oil nanofluids occurs at 412 °C [103]. The enhanced thermal resistance of the base fluid by nanoparticles will enable the fluid to operate at higher temperatures.

Summary of those evaluation methods

In order to summarize the above methods for measuring the stability of NFs, the principles and scope of application of the six methods are listed in the following table (Table 4).

Applications of solar nanofluids on heat collection

Now, reports on the utilization of NFs for solar energy collection have gradually increased. As non-polluting and plentiful energy, solar energy is favored by experts in the field of energy at home and abroad in solving the problem of global warming [105]. According to the data, the energy of solar radiation incident on the earth is about 1.7×10^{14} kW. Assuming that the solar energy can be used for only 84 min, it will greatly ease the consumption of global energy [106]. As an inexhaustible, clean and renewable energy, the efficient use of solar energy is of great significance for reducing the greenhouse effect and environmental pollution caused

by fossil fuels. Solar collectors which are commonly used in recent years include flat plate collectors, direct absorption collectors and parabolic trough collectors. Surface collectors heat the surface by absorbing solar radiation and transferring heat to the working fluid, while direct absorption collectors heat the working fluid by directly absorbing solar radiation. The core problem is that the working liquid used in solar collectors must have high heat transfer efficiency and light absorption capacity; therefore, NFs have been proposed for solar heat collection and a large number of experimental or theoretical studies have been carried out. Some experimental results have shown that the addition of trace amounts (ppm magnitude) of metals, oxides, CNTs, graphene, Au/TiN, TiN and other nanoparticles to fluids with water, oil, EG and other fluids can significantly improve the collector efficiency. We will refer to these NFs that can improve the heat collection efficiency as solar NFs, which are listed in Fig. 14.

Next, this paper will firstly study the heat transfer performance and light absorption characteristics of solar NFs, explore the operation mechanism of nanoparticles to improve the heat collection efficiency and finally summarize the current experimental applications of solar NFs.

Mechanism of heat collection of solar nanofluids

Achieving high-efficiency absorption, conversion and storage of solar radiation is a key goal in the field of solar thermal collection. Due to the lower specific heat of NFs, NFs can increase the collector outlet temperature higher than ordinary liquids under the condition of absorbing the same amount of solar radiation [1]. In addition, when NFs are used in direct absorption heat collectors, NFs with good properties of light absorption can broaden the absorption width of the solar spectrum and maximize the absorption efficiency of solar radiation. The high heat transfer efficiency of NFs also contributes to the conversion efficiency of solar radiation into thermal energy. These two features are described in detail below:

Optical properties of solar nanofluids

The solar radiation is mainly concentrated in the visible light part (0.4—0.76 μm), and less in range of the wavelengths of infrared rays (> 0.76 μm) longer than visible light and ultraviolet rays (< 0.4 μm). More than 99% of solar energy converge on wavelength from 0.15 to 4 μm , which are mainly distributed in the visible, infrared and ultraviolet regions, and which is about 3%, 44% and 53%, respectively [107]. Traditional fluids in solar collectors do not have broad spectral absorption properties, which limit the efficient heat collection of the system. Therefore, it is necessary to improve the fluid's absorption capacity in the visible and infrared regions, because more than 85% of the

Table 4 The summary of six methods measuring the stability of NFs

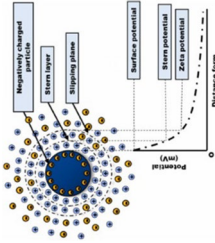
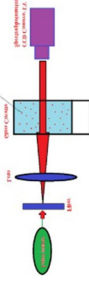
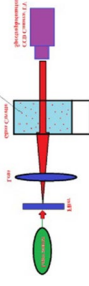

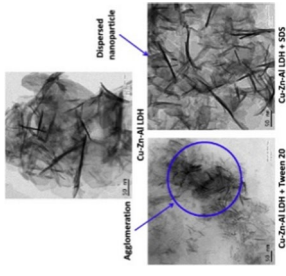
Method	Calculation formula	Schematic diagram	Conclusions
Zeta potential	$\mu_e = \frac{V}{E} \mu_e = \frac{2\epsilon_r \epsilon_0 f(\kappa a)}{3\eta}$	 <p>Electric double layer of particle. (Reprinted from ref [80], with permission from Elsevier)</p> 	<ol style="list-style-type: none"> 1. The absorbance decreases or the transmittance increases with time indicating an unstable NFs. 2. Limitations on the viscosity and concentration of NFs
Spectral absorbance and transmittance	$A_\lambda = \log(I_0/I) = \alpha \times l \times c$ $T_\lambda = I/I_0$	 <p>Schematic of the process. (Reprinted from ref [48], with permission from Elsevier)</p> 	<ol style="list-style-type: none"> 1. The absorbance decreases or the transmittance increases with time indicating an unstable NFs 2. Easy but take a long time
Sedimentation and centrifugation	$V_t = \frac{2r^2(\rho_p - \rho_b)g}{9\eta} V_t = \frac{d_p^2(\rho_p - \rho_b)\omega^2 X}{18\eta}$	<p>The sedimentation with time. (Reprinted from ref [82], with permission from Elsevier)</p>  <p>TEM image (Reprinted from ref [104], with permission from Elsevier)</p>	<ol style="list-style-type: none"> 1. The longer the suspension remains cloudy, the more stable it is 2. Easy but take a long time
TEM			<ol style="list-style-type: none"> 1. Can display visually the agglomeration 2. Easy to agglomerate during

Table 4 (continued)

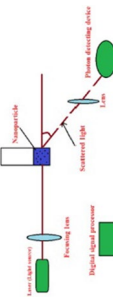
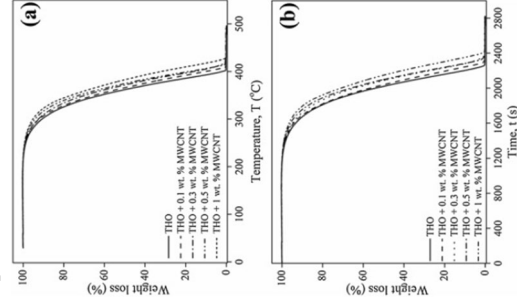
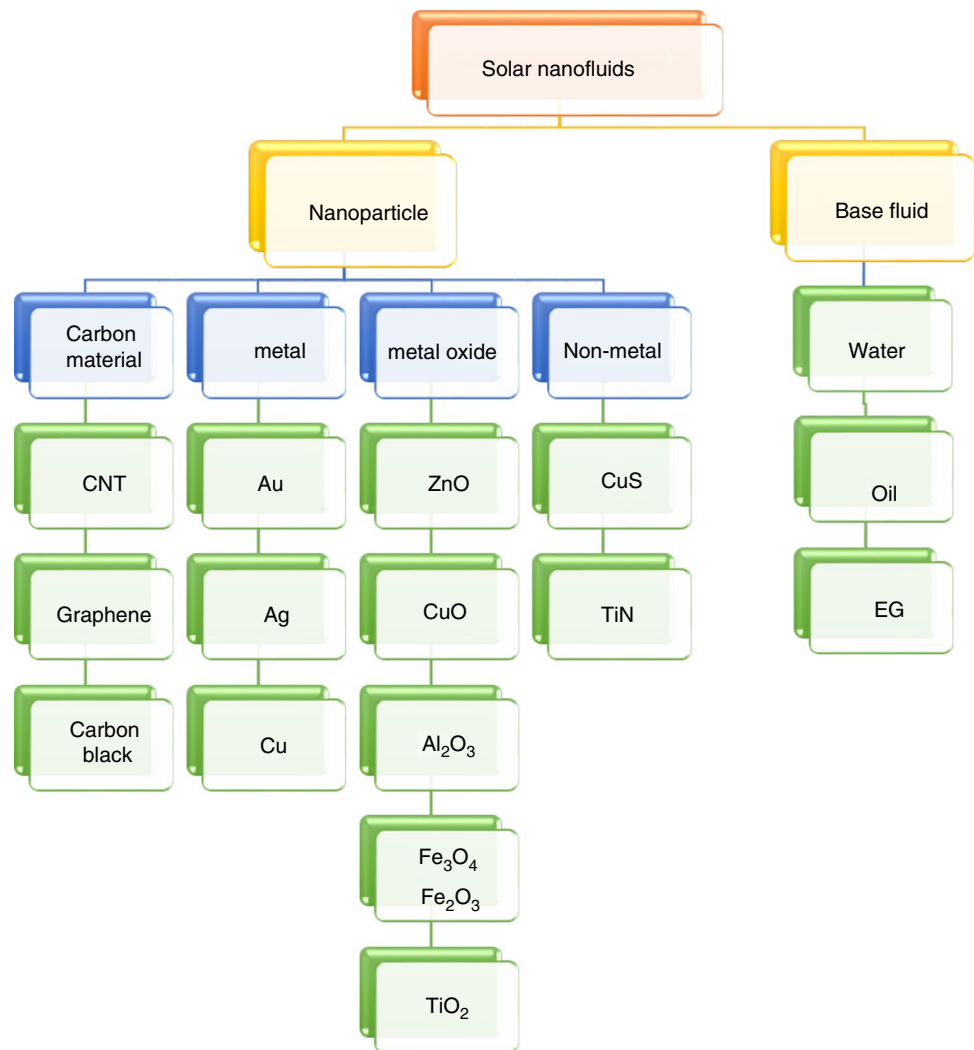
Method	Calculation formula	Schematic diagram	Conclusions
DLS	$R_H = \frac{k_B T}{6\pi\eta D}$	 <p>Schematic of the process (Reprinted from ref [48], with permission from Elsevier)</p>	<ol style="list-style-type: none"> 1. The diameter measured by DLS changed with time indicating unstable NFs 2. Not suitable for NFs with high concentration or multiple particle sizes
TGA		 <p>The TGA analysis of MWCNT NFs. (Reprinted from ref [103], with permission from Elsevier)</p>	<ol style="list-style-type: none"> 1. Emphasis is placed on measuring thermal stability

Fig. 14 The types of nanoparticles and base fluid to compose solar NFs

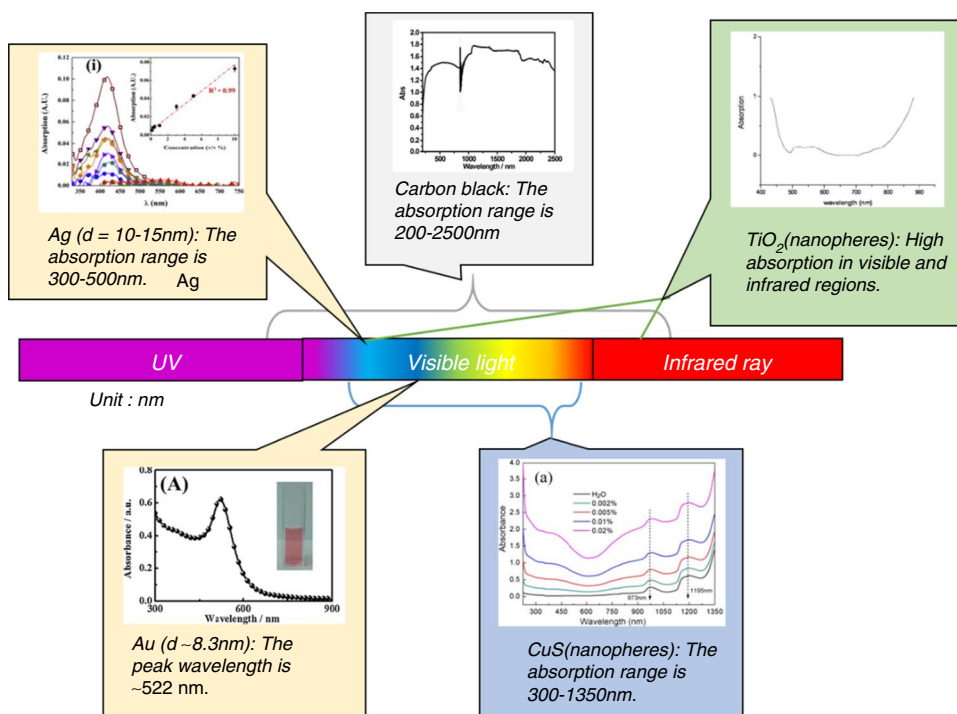


solar radiation energy is concentrated here. NFs are widely used in solar systems due to their ability to absorb specific solar spectrum, which helps to increase the temperature of NFs to produce high energy absorption capacity. Different types of NFs may obtain different absorption effects, and the spectral absorption properties of some solar NFs are shown in Fig. 15. Some studies have shown that factors such as the concentration and size of NFs can also affect the absorption of solar radiation [108]. And generally speaking, the relationship between absorbance and concentration satisfies the Beer law, showing a linear relationship, and the photo-thermal conversion efficiency of small-sized nanoparticles is better.

From the perspective of optical and thermos-physical properties, carbon materials are considered to be one of the most suitable materials for solar energy applications. Under the same exposure time, the temperature rise of amorphous carbon-based NFs is approximately three times that of distilled water [114]. In the ultraviolet–visible–near-infrared absorption spectrum, both water and carbon black NFs

have better absorption capacity in wavelength from 1400 to 2500 nm, while in the wavelength of 200–1400, carbon black NFs show better absorption than water. The low transmittance indicates that the carbon black nanofluids can absorb most solar energy in the whole wavelength about from 200 to 2500 nm [109]. Adding graphene and multi-walled carbon nanotubes to the fluid had the same effect. Compared with pure water, adding a small amount of N-(rGO-MWCNTs) to pure water can significantly improve the absorbance of the fluid, and with the increase in the concentration of nanoparticles, the optical absorption increases, and the peak of absorbance is around 272 nm. In addition, it was found that the light absorption ability of water-based NFs was stronger than that of EG-based NFs, and the enhancement rate of water-based NFs with a concentration of 0.02% was 2.6% higher than that of EG-based NFs with a volume fraction of 0.03% [115]. Lee et al. [116] experimented the absorbing ability of water-MWCNT NFs at a fixed wavelength of $k=632.8$ nm, and the results showed that the absorbing ability of MWCNT NFs upgraded linearly as the concentration

Fig. 15 The spectral absorption properties of some solar NFs, and those pictures come from [109–113]



increases. Not only that, at the depth of 10 cm, the water-MWCNT with only 0.0005 vol.% could completely absorb the incident solar energy of a fixed wavelength, reflecting the excellent light absorption performance of multi-walled carbon nanotube NFs.

Precious metal nanoparticles are also favored. These particles mainly rely on local surface ion resonance to achieve spectral absorption, and the spectral properties can be regulated by changing the shape and size of the particles [117]. Nanoparticles of different sizes have different absorption ranges. The Ag nanoparticles are divided into three types: type A (particle diameter is 10–50 nm), type B (particle diameter is 10–85 nm), and type C (particle diameter is 5–120 nm). The absorbance of A type NFs is mainly about 350–450 nm in wavelength, while B and C type is 350–800 nm. In particular, there is an absorption peak around 550 nm in the B-type nanofluids, probably due to the presence of larger nanoparticles (the diameter is range from 30 to 80 nm) [110]. Au NFs with a size ranging from 2 to 10 nm have an absorption peak around 528 nm and have good absorbance in the wavelength range of 300 to 600 nm [118]. Au and Ag nanoparticles appear to have similar light-absorbing properties. Au NFs with a concentration of 26 ppm (the diameter of Au nanoparticles are 24–38 nm) have high absorption rates on 200–700 nm, and high transmittance between 800 and 1100 nm, while Ag NFs (the diameter of Au nanoparticles are 16–23 nm) have high absorbance on 200–500 nm, and high transmittance between 700 and 1100 nm [117]. However, the size of the nanoparticles seems to be inversely related to the light absorptivity,

with the increase in the size of the Au nanoparticles, which changed from 62.1 nm to 170.6 nm, the absorptivity of the Au-water NFs decreases instead [111]. Quasi-spherical and spiny gold nanoparticles can be synthesized by a seed-mediated method. The wavelengths of the absorption peaks of the quasi-spherical and spiny NFs are located at 879–553 nm and 899–594 nm, respectively. As the gold nanoparticles changed from quasi-spherical to spiny, the absorption peak of the solar nanofluids on the spectrum changed from 562 to 772 nm, and the size of the gold nanoparticles in this experiment was 42~188 nm. The photo-thermal conversion efficiency of spiny gold NFs is also higher than that of quasi-spherical gold NFs [111, 119]. In particular, Zeiny et al. [118] compared the spectroscopic properties of gold, copper and carbon black NFs. The absorbance peak of copper NFs with a size of 10–30 nm measured by spectrometer is about 740 nm, which indicates that the absorption capacity of carbon black NFs is better than that of gold and copper NFs.

Metal oxide nanoparticles can also be utilized to strengthen the light absorption capacity of NFs in the visible or infrared region. The optical properties of CuO and ZnO-CuO binary water-based NFs were analyzed by spectrogram. The transmittances of the three NFs (CuO-ZnO binary NFs mixed in two different proportions) all decreased sharply with increasing concentrations, and at a concentration of 0.01%, the transmittance reaches zero, which achieved full absorption of sunlight. Compared with pure CuO, the binary oxide nanofluids exhibit an absorption peak at 368 nm. It can be seen that the addition of zinc oxide can improve the light absorption capacity at short wavelengths, and the

improvement increases with the increase in the addition amount [72]. The solar light absorptivity of TiO₂-water NFs which is 43 nm with 0.1 mass% showed a decreasing trend within the area of 440–500 nm, while there was an increasing trend in the wavelength range of 700–900 nm. TiO₂-water NFs exhibit good light absorption properties in the ultraviolet and infrared regions [113]. However, this is contrary to the results reported by Said et al. [120], TiO₂ NFs only have high absorption in the ultraviolet region and part of the visible light region, while the extinction coefficient in the infrared region is negligible. This may be due to the differences in the size of the prepared nanoparticles and the use of surfactants.

In addition to carbon materials, metals and metal oxides, other materials such as CuS and AlN also have good light absorption properties. For example, Fang et al. [112] tested the spectral absorption curve of water-CuS NFs with the volume fraction increased from 0.002% to 0.02%, and the results showed that CuS NFs have strong light absorption ability in the visible and near-infrared regions. Similarly, with the increase in concentration, the absorption rate also increased, and reached complete absorption at the concentration of 0.02%. In addition, they also verified that the light-absorbing ability of tubular NFs is stronger than that of spherical NFs, which may be due to the larger surface area or more slit-like pores of tubular nanoparticles. The AlN-water NFs exhibit partial absorption in the visible part, and the transmittance increases with wavelength increasing from 200 to 800 nm. In the spectral curve, TiN-water NFs have the strongest absorption capacity, whose transmittance was smaller than 1%, followed by ZrC-water NFs with solar radiation absorption capacity, whose transmittance was smaller than 8% [121].

The function of solar nanofluids on enhancing heat transfer

The high TC of NFs is also a key element to improve the heat collection efficiency of solar NFs. Brownian motion, clustering of particles, and thermophoresis are considered to be the main reasons for the strengthening of TC. Brownian motion refers to the phenomenon that when particles move in the base liquid, heat is transferred from one solid to another due to the collision effect, thereby realizing the enhancement of TC. The heat transfer process inside the NFs is affected by the generation of micro-convection due to the Brownian motion [122]. The aggregation of nanoparticles also helps to provide a transport path for heat inside the fluid [1]; however, the aggregation of particles to form bulky clusters is not conducive to the thermal conductivity of liquids. The other is the thermophoresis of nanoparticles. The nanoparticles act as the heat collector core. After the temperature rises, a non-uniform internal heat source term related to the optical thickness is added inside. The thermo-phoretic effect will cause the nanoparticles to migrate from the hot region to the cold region, thereby enhancing the convective heat transfer efficiency.

The addition of different types of nanoparticles can significantly improve the thermal conductivity of fluids, and many domestic and foreign scholars have carried out experimental research on this. Multi-walled carbon nanotubes are ideal materials for strengthening the heat transfer performance of liquids due to their high TC and large aspect ratio. As the SWCNT NFs' concentration varies from 0.05 vol.% to 0.25 vol.%, the thermal conductivity increases from 2.84% to 36.39% [123]. Compared with pure water, carbon nanotubes with a volume fraction of 0.05 vol.% can increase the thermal conductivity by 36% at 45 °C, which can be seen from Fig. 16 [124]. In addition to carbon materials, other nanoparticles such as metals and their oxides can improve

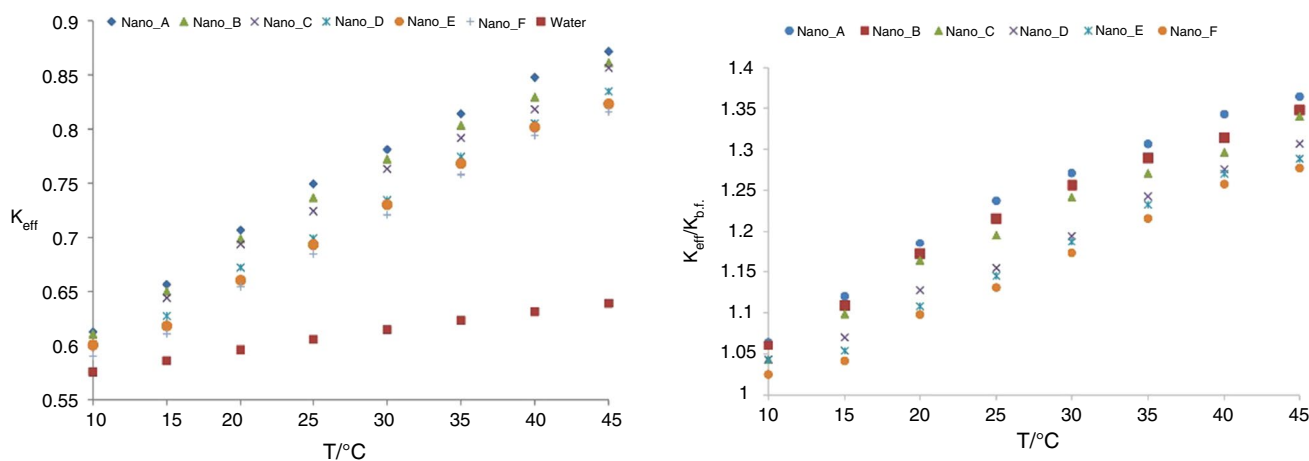


Fig. 16 The enhancement of thermal conductivity of pure water by CNTs. (Reprinted from ref [124], with permission from Elsevier)

thermal conductivity to varying degrees. The TiO₂-water nanofluids with a volume fraction of 3 vol.% can improve the thermal conductivity by 7.2% [73]. Al₂O₃-water NFs with a mass fraction of 0.15 mass% were reported to improve thermal conductivity by 10.1% [68]. Abareshi et al. [59] prepared magnetic Fe₃O₄ NFs by co-precipitation technology and measured its TC. The results indicated that at the temperature of 45°C, when the concentration is 3 vol.%, the highest strengthening rate of TC is 11.5%. The TC enhancement effect of solar NFs on different base fluids is different. CuO nanoparticles have a more apparent influence on improving the TC of distilled water, and the maximum enhancement rate can reach 40%, while the TC of EG and engine oil is weakly enhanced, increasing by 27% and 19%, respectively [58].

The efficiency of heat-collecting of nanofluids

Compared with pure water or other traditional industrial fluids, the unique optical properties of NFs can broaden the extinction spectrum of liquids, enhance the extinction ability in the visible or infrared region, and thus capture solar energy more efficiently. In addition, the high TC of the NFs further strengthens the heat transfer efficiency of the liquid and the solar collector. For example, the good light absorption properties and photothermal conversion properties of titanium nitride (TiN) materials have attracted the attention of some researchers. Wang et al. [125] analyzed the photothermal properties of TiN NFs. They experimented the influence of concentration on fluid warming: Below 500 ppm, the maximum temperature rise of TiN NFs increased with increasing concentration. When the concentration is higher than 500 ppm, the solar radiation is mainly absorbed by the surface of the fluid, which increases the heat dissipation of the surface temperature to the environment, while the heat transfer efficiency inside the fluid is lower than that of the surface, which increases heat loss. In addition, they compared the photothermal conversion efficiency of several common materials, and the heating rate was in the following order: TiN > Graphene > Au > CNTs-OH > Ag > CuS > EG. In particular, the maximum temperature rise of TiN within 20 min is 14.2 °C, which is 7 °C higher than that of graphene.

When the NFs are used in direct absorption solar collectors, the NFs act as both a heat collector and a heat transfer working fluid, and they exhibit efficient heat collection performance compared to traditional heat transfer working fluids. When 0.02 mass% MWCNTs nanofluids were placed under natural illumination, the nanofluids conversion efficiency reached 95% within the first 10 min. And with the increase in the concentration, the performance of the nanofluids does not decrease, which shows the great potential of carbon nanotubes for solar heat collection [126]. However,

with the increase in the concentration, there will be a large temperature difference between the upper and lower surfaces of the receiving end of the MWCNTs NFs, resulting in heat loss. To reduce the problem of heat loss caused by the uneven temperature distribution inside the receiver, the heat conduction inside the fluid can be changed into convection by adding a rotating magnetic field [127]. The experimental results show that the photothermal conversion efficiency of FeNi/C-EG NFs with a concentration of 50 ppm in direct absorption solar collectors can reach up to 58.7%, while the photo-thermal conversion efficiency of the non-external rotating magnetic field is 47.9%. When the concentration is increased from 5 to 50 ppm, the thermal conversion efficiency of the nanofluids with an external magnetic field can basically reach more than 50%. Based on the plasmonic effect of silver ions and the high thermal conductivity of carbon materials, Mehrali et al. [128] prepared reduced graphene oxide solar NFs modified by silver nanoparticles and used them to directly absorb solar heat collection devices. The study found that the Ag-rGO nanofluids can achieve a heat collection efficiency of up to 77% at a low concentration of 40 ppm, while the rGO nanofluids without modification by Ag ion reached the highest heat collection efficiency of 63.3% at the concentration of 80 ppm. It can be seen that the reduced graphene oxide NFs modified by silver ions can further strengthen the absorption ability of solar collectors. Similarly, they found that the temperature at the top of the fluid increased with increasing concentration, but the temperature at the lower surface of the liquid showed a different trend. Compared to pure water, NFs raise the temperature faster. CuO-water NFs, as solar absorbers, can be used for direct absorption parabolic trough solar collectors. When the nanofluids flow rate increased, the temperature difference parameters of nanofluids and pure water with volume fractions of 0.01 vol.%, 0.05 vol.% and 0.1 vol.% decreased by 68%, 67%, 65%, and 53%, respectively. In addition, the addition of CuO nanoparticles significantly improved the heat collection performance of the fluid, and the maximum increase in the thermal efficiency of the NFs with concentrations of 0.01%, 0.05% and 0.1% for pure water was 3.23 times, 3.6 times and 3.82 times, respectively [129].

Flat plate collectors are considered to be the most commonly used collectors, but due to their relatively low energy absorption and transfer efficiency, NFs have been proposed to replace traditional working fluids to strengthen the heat collection efficiency. When solar NFs work on flat-plate collectors, the main role is the high-efficiency heat transfer performance. Tong et al. [130] applied water, Al₂O₃, CuO, WO₃, MWCNT, and Fe₃O₄ NFs to flat-panel solar collectors and experimentally investigated their performance characteristics. The examinations display that the adjunction of nanoparticles significantly improves the heat collection efficiency of the fluid: when the working fluid is water, the

collector efficiency is only 62%, while when the working fluid is MWCNT, the collector efficiency increases to 87%. And carbon nanotube NFs are most sensitive to changes in solar radiation. In particular, they also found that the WO_3 nanofluids have the lowest heat loss coefficient and can maintain a good heat collection performance in a wider working range. Metal oxide NFs are a good choice for flat plate collectors. When the ZnO NFs work in the plate solar collector, the heat collection efficiency of the ZnO nanofluids with a volume fraction of 1 vol.% is 19.9% and 19.8% higher than that of the base fluid, respectively. Its highest efficiency can reach 70.28% and 69.24%, respectively. Its highest efficiency can reach 70.28% and 69.24%, respectively. When the volume fraction of MgO nanofluids is 0.2 vol.% and the flow rate is 1.5 Lit/min, the maximum thermal efficiency is 69.1%, which is 16.36% higher than that of EG/DW. However, when the flow rate is 1 Lit/min, the maximum thermal efficiency of the nanofluids can also reach 67.8%, which is not much different from that of the flow rate of 1.5 Lit/min [131]. The use of multi-walled carbon nanotubes can significantly improve the exergy efficiency and energy efficiency of the system. The maximum exergy efficiency of flat-panel solar collectors using NFs is about 23.35%, while the largest exergy efficiency using distilled water is 14.55%. Compared with pure water, the MWCNTs with concentrations of 0.01% mass%, 0.05 mass%, and 0.1 mass% increased the efficiency by 16%, 21%, and 34.13%, respectively. Based on the improvement of the heat collection efficiency, the collector no longer needs a large area size for solar radiation absorption, and 0.1 mass% MWCNTs can reduce the size of the flat plate collector by 34% [132]. Flat-plate collectors using hybrid NFs perform better than NFs alone: Hybrid NFs (covalently functionalized multi-walled carbon nanotubes and covalently functionalized graphene nanosheets) as interiors of flat-panel solar collectors. The thermal efficiency of the mixed nanofluids with a concentration of 0.10 mass% and a flow rate of 4 l/min is as high as 85%, which is 20% higher than that of DW at the same flow rate [133].

In addition to the most common flat plate collectors, the use of NFs in surface collectors such as parabolic trough and dish collectors also has good improvement effects. Khan et al. [134] used NFs for parabolic dish solar collectors combined with supercritical carbon dioxide Brayton cycles. Three oil-based NFs (Al_2O_3 , CuO and TiO_2) were used in this collector, and the experiments displayed that the total energy efficiency and exergy efficiency of Al_2O_3 oil-based NFs were the highest, and TiO_2 /oil-based NFs was higher than CuO/oil-based NFs. As the mass flow rate of the nanofluids ($0.1\text{--}0.3\text{ kg s}^{-1}$) increases, the system efficiency increases significantly, but the lift effect slows down after 0.3 kg s^{-1} . Specially, the working fluid of the parabolic trough collector can be gas, and the gas can work at a higher

temperature than the liquid. The air dispersed with CuO powder is used for the high-temperature parabolic trough collector, the maximum temperature of the fluid can reach $180\text{ }^\circ\text{C}$ within 24 h, and the fluid temperature above $145\text{ }^\circ\text{C}$ is maintained for about 10 h, and the average efficiency of the parabolic trough collector is 65% [135].

The efficiency heat collection of volumetric solar collectors is generally higher than that of surface collectors. Lee et al. [136] systematically investigated the heat collection efficiency of surface solar collectors and nanofluids-based volumetric solar collectors. They prepared stable carbon nanotube NFs with different volume fractions (0.0005~0.005 vol.%), and analyzed the heat collection efficiencies of the two solar collectors according to volume fractions and Peclet numbers. The results showed that the volumetric solar collectors with nanofluids have higher heat collection efficiency, which is 10% higher than that of conventional surface solar collectors.

To sum up, nanomaterials with good optical properties and heat transfer properties, such as MWCNT, TiN, Au, Cu, CuO, ZnO, Al_2O_3 , etc., are used in solar collectors to significantly improve the heat collection efficiency. Relatively speaking, carbon materials with high thermal conductivity (MWCNT, graphene) have more efficient heat collection properties, and in particular, TiN materials also exhibit excellent photothermal properties. Based on the analysis above, the reason why solar nanofluids can improve the efficiency of solar energy collectors is that they have a longer spectral absorption band and better thermal conductivity, especially metal nanoparticles have better optical absorption properties due to the plasmon resonance effect. Many researchers have used mixed nanofluids containing metal particles and other non-metallic nanoparticles to achieve full spectrum absorption to improve heat collection efficiency. However, in the direct absorption solar collector, as the concentration increases, the heat collection efficiency also increases, but at the same time, the heat loss also increases. The reason is that the increase in the concentration causes the temperature of the fluid surface to rise rapidly, which causes the heat dissipation of the upper surface to the surrounding environment to be accelerated. Some studies have shown that the heat loss caused by this reason can be effectively reduced by applying an external magnetic field.

Compared with surface solar collectors, volumetric solar collectors can make the most of the properties of nanomaterials. NFs can be used as working fluids to directly absorb solar energy, which can not only strengthen the absorption of solar radiation in the visible or infrared region, but also enhance the heat transfer efficiency inside the fluid, and improve the collector efficiency from both solar energy absorption and transmission. In surface collectors, the only thing that plays the biggest role is the enhancement of the thermal conductivity of the base liquid by nanomaterials.

Table 5 Research on application of nanofluids on collecting solar energy

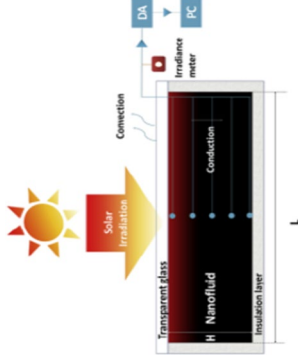
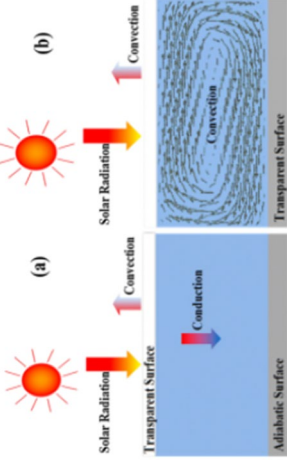
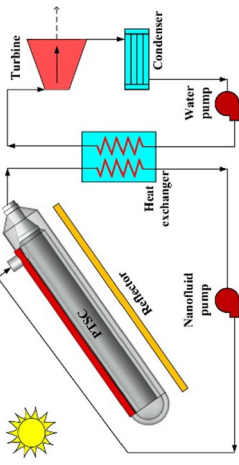
Author	System of heat collection	Type of nanofluids	Concentration	Main conclusions
Chen et al. [126]		MWCNTs-water	0.001–0.02 mass%	Obtained a photothermal conversion efficiency of 95% in the first 10 min with concentration of 0.02mass%
Wang et al. [127]	<p>Test device for photothermal properties of NFs</p> 	FeNi/C-EG	5–50 ppm	Combined with the rotating magnetic field, the photothermal conversion efficiency is enhanced to 58.1%. At 50 ppm, the rotating magnetic field increases by 22.7%
Yang et al. [137]	<p>Traditional & rotary magnetic field</p> 	Al ₂ O ₃ -oil	1–4 vol %	Nanofluids trough collector system with preheat and top cover can improve PEC index by up to 53% and significantly reduce investment cost

Table 5 (continued)

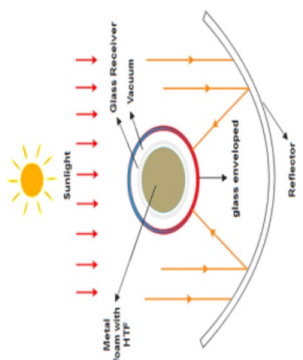
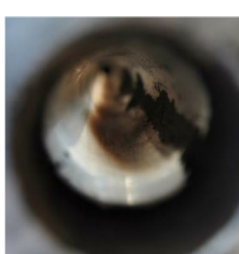
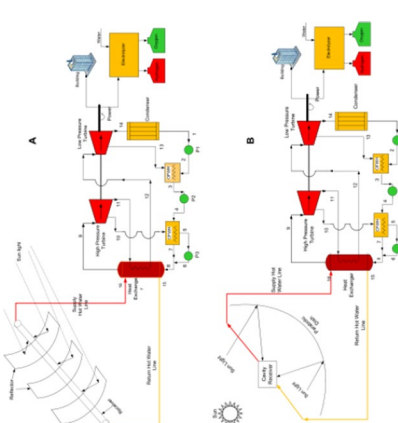
Author	System of heat collection	Type of nanofluids	Concentration	Main conclusions
Heyhat et al. [129]	 <p>Direct absorption parabolic trough solar collector</p>	CuO-water	0.01–0.1 vol. %	The maximum thermal efficiency of 0.01%, 0.05% and 0.1% CuO NFs is 3.23 times, 3.6 times and 3.82 times that of pure water, respectively. The composite use with metal foam can further improve the efficiency
Potenza et al. [135]	 <p>Parabolic trough collector with photograph of deposition of nanoparticles</p>	CuO-air	0.01–0.3 vol. %	Using CuO-air nanofluids as the working fluid, in one day's measurement, the fluid temperature was maintained above 145 °C for about 10 h, and the maximum reached 180 °C, with an average efficiency of about 65%
Abid et al. [139]	 <p>Solar thermal power system a) trough type, b) dish type</p>	Al ₂ O ₃ , Fe ₂ O ₃ -water	0–0.3%	NFs have better overall performance, net power and hydrogen production rate

Table 5 (continued)

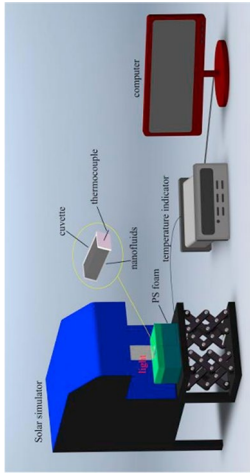
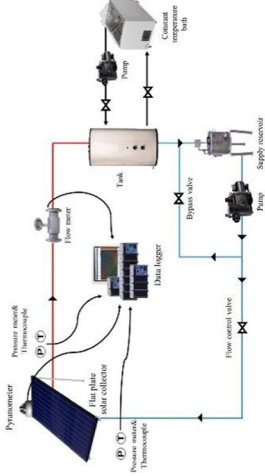
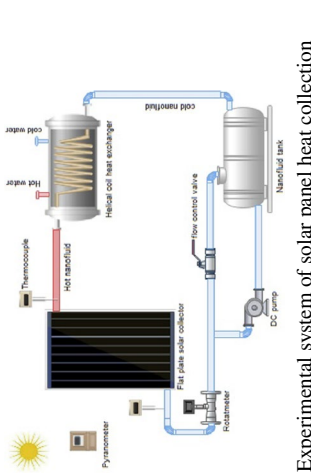
Author	System of heat collection	Type of nanofluids	Concentration	Main conclusions
Wang et al. [125]	 <p>System flow of photothermal conversion experiment</p>	Plasmons Au/TiN, TiN, CNTs, EG	10–100 ppm	Photo-thermal efficiency: plasmonic Au/TiN > TiN > graphene > Au > CNTs > Ag > CuS > EG, the optimal concentration of plasmonic Au/TiN is 100 ppm
Tong et al. [130]	 <p>System flow of photothermal conversion experiment</p>	Al_2O_3 , CuO, Fe_3O_4 , CeO_2 , MWCNT, WO_3 -water	0.005–1 vol. %	Heat collecting efficiency: 1% Al_2O_3 increased by 3.8%, 0.5% CuO increased by 4%, 0.005% Fe_3O_4 increased by 3%, 0.0015% MWCNT increased by 8.8%
Choudhary et al. [131, 140]	 <p>System flow of photothermal conversion experiment</p> <p>Experimental system of solar panel heat collection</p>	ZnO, MgO-water	0.08–1 vol. %	1% ZnO improves the heat collection efficiency by 19.2% and reduces heat loss by 62.5%; 2% MgO improves heat collection efficiency by 16.7% and reduces heat loss by 52.2%;

Table 5 (continued)

Author	System of heat collection	Type of nanofluids	Concentration	Main conclusions
Eltaee-land [132]	<p>1. Flat-plate collector 2. Tank 3. Pump 4. Heat exchanger 5. Storage tank</p>	MWCNTs-water	0.01–0.1 mass%	Heat collection performance: 0.01% increased by 16%, 0.05% increased by 21%, 0.1% increased by 34.13%
Husseind et al. [133]	<p>Photographs of experimental system of solar panel heat collection</p>	Covalently functionalized MWCNTs + GNPs + h-BN-water	0.05–0.1 mass%	The performance of the mixture with three kinds is the best: 0.05% improved the heat collection efficiency by 11.8%, and 0.1% improved the heat collection efficiency by 21.9%

Experimental system of solar panel heat collection

The relevant literature on the use of NFs for solar heat collection is summarized in Table 5 as follows.

Conclusions

Many research focused on solar collectors, and the NFs are widely used as working fluids seen from those researches. However, the reviews specifically for solar nanofluids that can absorb solar radiation have been rarely reported. Most of the literature focuses on the upgrade of the structure of solar collectors, but the enhancement mechanism and heat collection effect of solar nanofluids are lacking. Hence, it is necessary to supplement the performance of solar nanofluids themselves. In this paper, we analyzed the stability mechanism of solar nanofluids, and then assessed various methods for preparing long-term stable solar nanofluids and their characterization methods. Finally, the applications of solar nanofluids in heat collection systems were summarized. The main conclusions are as follows:

The commonly used nanofluids preparation techniques are the one-step method and the two-step method, and the advantages and disadvantages of the two methods are actually complementary. The nanofluids particles prepared by the one-step method are smaller and more precise, and the nanofluids have better stability, but the economic cost is huge. The two-step method for synthesizing NFs is technically simple and can industrially produce nano-powders, but the stability of NFs cannot be guaranteed, so the prepared NFs can only be used in experiments. In order to prepare long-term stable nanofluids, reducing the cost of the one-step method or using other methods to improve the stability of nanofluids prepared by two-step methods will be the focus of future research.

Compared with solar collectors using pure water, the reasons why solar collectors using NFs can significantly improve the efficiency of solar heat collection are at two points:

- Nanoparticles have a strong light absorption ability in the visible light region, and 44% of the energy of solar radiation is concentrated in this region, which can maximize the solar energy absorption efficiency of solar energy.
- Nanoparticles can effectively improve the thermal conductivity of the fluid, so that the thermal energy can be rapidly transferred in the fluid, and the solar energy conversion and transportation capacity of the collector can be improved.

In future work, it may become the focus to compare multiple solar nanofluids in solar collectors to maximize the efficiency of the heat-collection system. In addition, how to

avoid the deposition, blockage and erosion of nanofluids is also something that researchers should consider.

Knowledge gaps and future challenges

This paper provides a necessary review of the preparation, stability and applications on solar heat collection of solar NFs. After a comprehensive analysis of the preparation technology, evaluation technology of stability, and thermal collection efficiency of solar NFs, this paper gives the following suggestions for the current knowledge gap and future development of NFs:

Knowledge gaps on stability

- Long-term stability is essential for the application of NFs to heat collector systems or other projects. Considering the cost, the two-step preparation technique is widely used, but this makes the NFs easily agglomerate or settle. The nanoparticles will precipitate in the pipeline, and the presence of solids will block the operation of the system, which greatly reduces the service life of the system. In addition, the production cost of NFs is too high, and it is still unable to completely replace the status of traditional working fluids in terms of economic benefits.
- The current detection methods for stability are mostly carried out in the initial period or short experimental cycle after the completion of the preparation of NFs, lacking long-term systematic detection methods for the stability of NFs. And practical detection methods such as the zeta potential method have the possibility of misjudging the stability of NFs.
- At present, there is still a big gap in the study of the stability of NFs, and the establishment of theoretical models needs to be further developed.

Applications on heat-collecting

- About the long-term observation and evaluation of the system of solar collectors are lacked. The corrosion of NFs to the system, the blockage caused by precipitation or the reduction in the overall efficiency of the system caused by the reduction in the heat-collecting load capacity of particles still requires a lot of experiments.
- Under intense UV irradiation, solar radiation may negatively affect the chemical stability of NFs, which requires further experimental exploration. In addition, how to detect the chemical stability of NFs and prevent chemical instability caused by prolonged exposure to ultraviolet light is also an urgent problem to be settled.
- It can be seen from a large number of experimental reports that the increase in the concentration of NFs will

cause unnecessary heat loss due to a surface temperature of the fluid which is much higher than the ambient temperature. This may be one of the bottlenecks that limit the further improvement of the efficiency of collectors with nanofluids.

Negative impact of nanofluids

It is reported that nanoparticles may make a positive contribution to the rate of bacterial mutation [141]. Nanoparticles may cause pollution to the environment during production, storage, transportation, etc. As we all know, particles under 10 μm can be inhaled by the human body, while nanoparticles with a size of only 1–100 nm can completely enter the human body through the respiratory tract and pose a threat to life and health.

Acknowledgements The work of this paper is financially supported by the National Natural Science Foundation of China (52176061, 51876040), the Scientific and Technological Innovation Project of Carbon Emission Peak and Carbon Neutrality of Jiangsu Province (No. BE2022028–4), and the Project of Jiangsu Provincial Six Talent Peaks. The supports are gratefully acknowledged.

References

1. Tembhare SP, Barai DP, Bhanvase BA. Performance evaluation of nanofluids in solar thermal and solar photovoltaic systems: a comprehensive review. *Renew Sust Energy Rev.* 2022;153:111738. <https://doi.org/10.1016/j.rser.2021.111738>.
2. Shahzad M, Ma T, Jurasz J, Canales FA, Lin S, Ahmed S, et al. Economic analysis and optimization of a renewable energy based power supply system with different energy storages for a remote island. *Renew Energy.* 2021;164:1376–94. <https://doi.org/10.1016/j.renene.2020.10.063>.
3. Kalvin R, Taweekun J, Maliwan K, Ali HM. Fabrication of catalytic converter with different materials and comparison with existing materials in addition to analysis of turbine installed at the exhaust of 4 stroke SI engine. *Sustainability.* 2021;13(18):10470.
4. Sheikholeslami M. Analyzing melting process of paraffin through the heat storage with honeycomb configuration utilizing nanoparticles. *J Energy Storage.* 2022;52:104954. <https://doi.org/10.1016/j.est.2022.104954>.
5. Rodriguez-Sanchez D, Belmonte JF, Izquierdo-Barrimentos MA, Molina AE, Rosengarten G, Almendros-Ibáñez JA. Solar energy captured by a curved collector designed for architectural integration. *Appl Energy.* 2014;116:66–75.
6. Tian Y, Zhao CY. A review of solar collectors and thermal energy storage in solar thermal applications. *Appl Energy.* 2013;104:538–53. <https://doi.org/10.1016/j.apenergy.2012.11.051>.
7. Saidur R, Meng TC, Said Z, Hasanuzzaman M, Kamyar A. International journal of heat and mass transfer evaluation of the effect of nanofluid-based absorbers on direct solar collector. *Int J Heat Mass Transf.* 2012;55:5899–907. <https://doi.org/10.1016/j.ijheatmasstransfer.2012.05.087>.
8. Ruhani B, Barnoon P, Toghraie D. Statistical investigation for developing a new model for rheological behavior of Silica – ethylene glycol / Water hybrid Newtonian nanofluid using experimental data. *Physica A.* 2019;525:616–27. <https://doi.org/10.1016/j.physa.2019.03.119>.
9. Sajjad U, Sadeghianjahromi A, Muhammad H, Wang C. Enhanced pool boiling of dielectric and highly wetting liquids – A review on surface engineering. *Appl Therm Eng.* 2021;195:117074. <https://doi.org/10.1016/j.applthermaleng.2021.117074>.
10. Sheikholeslami M. Solar Energy Materials and Solar Cells Numerical investigation of solar system equipped with innovative turbulator and hybrid nanofluid. *Sol Energy Mater Sol Cells.* 2022;243:111786. <https://doi.org/10.1016/j.solmat.2022.111786>.
11. Masoud S, Yazdani A, Dhahad H, Alawee WH, Hesabi S, Norozpour F, et al. Effect of Ag, Au, TiO₂ metallic / metal oxide nanoparticles in double-slope solar stills via thermodynamic and environmental analysis. *J Clean Prod.* 2021;311:127689. <https://doi.org/10.1016/j.jclepro.2021.127689>.
12. Li Z, Barnoon P, Toghraie D, Balali R, Afrand M. Mixed convection of non-Newtonian nanofluid in an H-shaped cavity with cooler and heater cylinders filled by a porous material: two phase approach. *Adv Powder Technol.* 2019;30:2666–85. <https://doi.org/10.1016/j.appt.2019.08.014>.
13. Kavusi H, Toghraie D. A comprehensive study of the performance of a heat pipe by using of various nanofluids. *Adv Powder Technol.* 2017;28:3074–84. <https://doi.org/10.1016/j.appt.2017.09.022>.
14. Mashayekhi R, Khodabandeh E, Ali O, Davood A. CFD analysis of thermal and hydrodynamic characteristics of hybrid nanofluid in a new designed sinusoidal double-layered microchannel heat sink. *J Therm Anal Calorim.* 2018;134:2305–15. <https://doi.org/10.1007/s10973-018-7671-3>.
15. Bazdar H, Toghraie D, Pourfattah F, Ali O, Hoang A, Nguyen M. Numerical investigation of turbulent flow and heat transfer of nanofluid inside a wavy microchannel with different wavelengths. *J Therm Anal Calorim.* 2020;139:2365–80. <https://doi.org/10.1007/s10973-019-08637-3>.
16. Tariq HA, Anwar M, Malik A, Ali HM. Hydro-thermal performance of normal-channel facile heat sink using TiO₂-H₂O mixture (Rutile–Anatase) nanofluids for microprocessor cooling. *J Therm Anal Calorim.* 2021;145(5):2487–502. <https://doi.org/10.1007/s10973-020-09838-x>.
17. Choi SUS, Eastman JA. Enhancing thermal conductivity of fluids with nanoparticles. *Asme Fed 231* (1995), 99–105.
18. Liu J, Ye Z, Zhang L, Fang X, Zhang Z. Solar energy materials & solar cells a combined numerical and experimental study on graphene / ionic liquid nano fluid based direct absorption solar collector. *Sol Energy Mater Sol Cells.* 2015;136:177–86. <https://doi.org/10.1016/j.solmat.2015.01.013>.
19. Chen W, Chou H, Yang Y. Inverse estimation of the unknown base heat flux in irregular fins made of functionally graded materials. *Int Commun Heat Mass Transf.* 2017;87:157–63. <https://doi.org/10.1016/j.icheatmasstransfer.2017.07.003>.
20. Sharaf OZ, Taylor RA, Abu-nada E. On the colloidal and chemical stability of solar nanofluids: from nanoscale interactions to recent advances. *Phys Rep.* 2020;867:1–84. <https://doi.org/10.1016/j.physrep.2020.04.005>.
21. Anderson A, Brindhadevi K, Salmen SH, Alahmadi TA, Marouskova A, Sangeetha M, et al. Effects of nanofluids on the photovoltaic thermal system for hydrogen production via electrolysis process. *Int J Hydrog Energy.* 2022. <https://doi.org/10.1016/j.ijhydene.2021.12.218>.
22. Abdelkareem MA, Maghrabie HM, Abo-Khalil AG, Adhari OHK, Sayed ET, Radwan A, et al. Battery thermal management systems based on nanofluids for electric vehicles. *J Energy Storage.* 2022;50:104385. <https://doi.org/10.1016/j.est.2022.104385>.
23. Yang X, Zhao Z, Liu Y, Xing R, Sun Y. Simulation of nanofluid-cooled lithium-ion battery during charging: a battery connected

- to a solar cell. *Int J Mech Sci.* 2021;212:106836. <https://doi.org/10.1016/j.ijmecsci.2021.106836>.
24. Gupta SK, Pradhan S. A review of recent advances and the role of nanofluid in solar photovoltaic thermal (PV/T) system. *Mater Today Proc.* 2021;44:782–91. <https://doi.org/10.1016/j.matpr.2020.10.708>.
 25. Jannen A, Chaabane M, Mhiri H, Bournot P. Performance enhancement of concentrated photovoltaic systems CPVS using a nanofluid optical filter. *Case Studies Therm Eng.* 2022;35:102081. <https://doi.org/10.1016/j.csite.2022.102081>.
 26. Sheikholeslami M, Ebrahimpour Z. International Journal of Thermal Sciences Thermal improvement of linear Fresnel solar system utilizing Al₂O₃-water nanofluid and multi-way twisted tape. *Int J Therm Sci.* 2022;176:107505. <https://doi.org/10.1016/j.ijthermalsci.2022.107505>.
 27. Hu G, Ning X, Hussain M, Sajjad U, Sultan M, Muhammad H, et al. Potential evaluation of hybrid nanofluids for solar thermal energy harvesting: a review of recent advances. *Sust Energy Technol Assess.* 2021;48:101651. <https://doi.org/10.1016/j.seta.2021.101651>.
 28. Sheikholeslami M, Farshad SA. Nanoparticles transportation with turbulent regime through a solar collector with helical tapes. *Adv Powder Technol.* 2022;33:103510. <https://doi.org/10.1016/j.apt.2022.103510>.
 29. Ahmed MS, Elsaid AM. Effect of hybrid and single nanofluids on the performance characteristics of chilled water air conditioning system. *Appl Therm Eng.* 2019;163:114398. <https://doi.org/10.1016/j.applthermaleng.2019.114398>.
 30. Sheikholeslami M, Said Z, Jafaryar M. Hydrothermal analysis for a parabolic solar unit with wavy absorber pipe and nano fluid. *Renew Energy.* 2022;188:922–32. <https://doi.org/10.1016/j.renene.2022.02.086>.
 31. Sheikholeslami M, Jafaryar M, Gerdroodbary MB. Environmental Technology & Innovation Influence of novel turbulator on efficiency of solar collector system. *Environ Technol Innov.* 2022;26:102383. <https://doi.org/10.1016/j.eti.2022.102383>.
 32. Yang L, Hu Y. Toward TiO₂ nanofluids—part I: preparation and properties. *Nanoscale Res Lett.* 2017;12(1):1–21.
 33. Yang L, Huang JN, Ji W, Mao M. Investigations of a new combined application of nanofluids in heat recovery and air purification. *Powder Technol.* 2020;360:956–66.
 34. Kumar P, Sarviya RM. Materials today : proceedings recent developments in preparation of nanofluid for heat transfer enhancement in heat exchangers: a review. *Mater Today Proc.* 2021;44:2356–61. <https://doi.org/10.1016/j.matpr.2020.12.434>.
 35. Jurčević M, Nižetić S, Arıcı M, Ocloń P. Comprehensive analysis of preparation strategies for phase change nanocomposites and nanofluids with brief overview of safety equipment. *J Clean Prod.* 2020;274:122963.
 36. Wang G, Li Y, Wang E, Huang Q, Wang S, Li H. International journal of mining science and technology experimental study on preparation of nanoparticle-surfactant nanofluids and their effects on coal surface wettability. *Int J Min Sci Technol.* 2021. <https://doi.org/10.1016/j.ijmst.2021.12.007>.
 37. Yang L, Jiang W, Ji W, Mahian O, Bazri S, Sadri R. International journal of heat and mass transfer a review of heating / cooling processes using nanomaterials suspended in refrigerants and lubricants. *Int J Heat Mass Transf.* 2020;153:119611. <https://doi.org/10.1016/j.ijheatmasstransfer.2020.119611>.
 38. Zhang J, Luo X, Wang L, Feng Z, Li T. Combined effect of electric field and nanofluid on bubble behaviors and heat transfer in flow boiling of minichannels. *Powder Technol.* 2022;408:117743. <https://doi.org/10.1016/j.powtec.2022.117743>.
 39. Rios MSBL, Rivera-solorio CI, Nigam KDP. An overview of sustainability of heat exchangers and solar thermal applications with nanofluids: a review organic rankine cycle. *Renew Sust Energy Rev.* 2021;142:110855. <https://doi.org/10.1016/j.rser.2021.110855>.
 40. Baktavatchalam B, Habib K, Saidur R, Saha BB. Cooling performance analysis of nanofluid assisted novel photovoltaic thermoelectric air conditioner for energy efficient buildings. *Appl Therm Eng.* 2022. <https://doi.org/10.1016/j.applthermaleng.2022.118691>.
 41. Wahab A, Hassan A, Qasim MA, Ali HM, Babar H, Sajid MU. Solar energy systems—potential of nanofluids. *J Mol Liq.* 2019;289:111049.
 42. Borode A, Ahmed N, Olubambi P. A review of solar collectors using carbon-based nanofluids. *J Clean Prod.* 2019;241:118311. <https://doi.org/10.1016/j.jclepro.2019.118311>.
 43. Lee GJ, Kim CK, Lee MK, Rhee CK, Kim S, Kim C. Thermal conductivity enhancement of ZnO nanofluid using a one-step physical method. *Thermochim Acta.* 2012;542:24–7. <https://doi.org/10.1016/j.tca.2012.01.010>.
 44. Khoshvaght-aliabadi M, Eskandari M. Influence of twist length variations on thermal – hydraulic specifications of twisted-tape inserts in presence of Cu – water nanofluid. *Exper Therm Fluid Sci.* 2015;61:230–40. <https://doi.org/10.1016/j.expthermflusci.2014.11.004>.
 45. Zhu HT, Lin YS, Yin YS. A novel one-step chemical method for preparation of copper nanofluids. *J Colloid Interface Sci.* 2004;277(1):100–3.
 46. Zhu H, Zhang C, Liu S, Tang Y, Yin Y. Effects of nanoparticle clustering and alignment on thermal conductivities of Fe₃O₄ aqueous nanofluids. *Appl Phys Lett.* 2006;89(2):023123.
 47. Chaturvedi KR, Sharma T. Journal of petroleum science and engineering rheological analysis and EOR potential of surfactant treated single-step silica nanofluid at high temperature and salinity. *J Petrol Sci Eng.* 2021;196:107704. <https://doi.org/10.1016/j.petrol.2020.107704>.
 48. Kiani MR, Meshksar M, Makarem MA, Rahimpour MR. Preparation, stability, and characterization of nanofluids. Berlin: Nano-fluids and Mass Transfer Elsevier; 2022.
 49. Salari S, Jafari SM. Trends in food science & technology application of nanofluids for thermal processing of food products. *Trends Food Sci Technol.* 2020;97:100–13. <https://doi.org/10.1016/j.tifs.2020.01.004>.
 50. Pazdar S, Sartipzadeh O. Experimental investigation of water based nano fluid containing copper nanoparticles across helical microtubes ☆. *Int Commun Heat Mass Transf.* 2016;70:84–92. <https://doi.org/10.1016/j.icheatmasstransfer.2015.12.006>.
 51. Kumar SA, Meenakshi KS, Narashimhan BRV, Srikanth S, Artanareeswaran GJMC. Synthesis and characterization of copper nanofluid by a novel one-step method. *Mater Chem Phys.* 2009;113(1):57–62.
 52. Salehi JM, Heyhat MM, Rajabpour A. Enhancement of thermal conductivity of silver nanofluid synthesized by a one-step method with the effect of polyvinylpyrrolidone on thermal behavior. *Appl Phys Lett.* 2013;102(23):231907.
 53. Singh AK, Raykar VS. Microwave synthesis of silver nanofluids with polyvinylpyrrolidone (PVP) and their transport properties. *Colloid Polymer Sci.* 2008;286(14):1667–73.
 54. Bönnemann H, Botha SS, Bladergroen B, Linkov VM. Monodisperse copper-and silver-nanocolloids suitable for heat-conductive fluids. *Appl Organomet Chem.* 2005;19(6):768–73.
 55. Teng T, Lin L, Yu C. Preparation and characterization of carbon nanofluids by using a revised water-assisted synthesis method. *J Nanomater.* 2013. <https://doi.org/10.1155/2013/582304>.
 56. Lo CH, Tsung TT, Chen LC, Su CH, Lin HM. Fabrication of copper oxide nanofluid using submerged arc nanoparticle synthesis system (SANSS). *J Nanoparticle Res.* 2005;7(2):313–20.
 57. Hung Y, Teng T, Lin B. Evaluation of the thermal performance of a heat pipe using alumina nanofluids. *Exp Therm Fluid Sci.*

- 2013;44:504–11. <https://doi.org/10.1016/j.expthermflusci.2012.08.012>.
58. Agarwal R, Verma K, Kumar N, Kumar R. Synthesis, characterization, thermal conductivity and sensitivity of CuO nanofluids. *Appl Therm Eng.* 2016;102:1024–36. <https://doi.org/10.1016/j.applthermaleng.2016.04.051>.
 59. Abareshi M, Goharshadi EK, Mojtaba S. Journal of magnetism and magnetic materials fabrication, characterization and measurement of thermal conductivity of Fe₃O₄ nanofluids. *J Magn Magn Mater.* 2010;322:3895–901. <https://doi.org/10.1016/j.jmmm.2010.08.016>.
 60. Liu MS, Lin MCC, Huang IT, Wang CC. Enhancement of thermal conductivity with carbon nanotube for nanofluids. *Int Commun Heat Mass Transf.* 2005;32(9):1202–10.
 61. Kathiravan R, Kumar R, Gupta A, Chandra R. Preparation and pool boiling characteristics of copper nanofluids over a flat plate heater. *Int J Heat Mass Transf.* 2010;53:1673–81. <https://doi.org/10.1016/j.ijheatmasstransfer.2010.01.022>.
 62. Qu J, Wu H, Cheng P. Thermal performance of an oscillating heat pipe with Al₂O₃ – water nano fluids ☆. *Int Commun Heat Mass Transf.* 2010;37:111–5. <https://doi.org/10.1016/j.icheatmasstransfer.2009.10.001>.
 63. Vermahmoudi Y, Peyghambarzadeh SM, Hashemabadi SH, Naraki M. Experimental investigation on heat transfer performance of Fe₂O₃ / water nanofluid in an air-finned heat exchanger. *Europ J Mech B/Fluids.* 2014;44:32–41. <https://doi.org/10.1016/j.euromechflu.2013.10.002>.
 64. Xuan Y, Li Q. Heat transfer enhancement of nanofluids. *Int J Heat Fluid Flow.* 2000;21:58–64.
 65. Choi SUS, Zhang ZG, Yu W, Lockwood F E, Grulke E A. Anomalous thermal conductivity enhancement in nanotube suspensions. *Appl phys lett.* 2001;79(14):2252–4.
 66. Xie H, Lee H, Youn W, Choi M. Nanofluids containing multi-walled carbon nanotubes and their enhanced thermal conductivities. *J Appl phys.* 2003;94(8):4967–71.
 67. Gharagozloo PE, Goodson KE. Dependent aggregation and diffusion in nanofluids. *Int J Heat Mass Transf.* 2011;54:797–806. <https://doi.org/10.1016/j.ijheatmasstransfer.2010.06.058>.
 68. Zhu D, Li X, Wang N, Wang X, Gao J, Li H. Dispersion behavior and thermal conductivity characteristics of Al₂O₃–H₂O nanofluids. *Curr Appl Phys.* 2009;9(1):131–9.
 69. Cacia K, Ordoñez F, Zapata C, Herrera B, Pabón E, Buitrago-Sierra R. Surfactant concentration and pH effects on the zeta potential values of alumina nanofluids to inspect stability. *Colloids Surf A Physicochem Eng Asp.* 2019;583:123960.
 70. Kole M, Dey TK. Thermophysical and pool boiling characteristics of ZnO-ethylene glycol nano fluids. *Int J Therm Sci.* 2012;62:61–70. <https://doi.org/10.1016/j.ijthermalsci.2012.02.002>.
 71. Peyghambarzadeh ESSM, Hormozi MMSF, Deionized DI. Thermal behavior of aqueous iron oxide nano - fluid as a coolant on a flat disc heater under the pool boiling condition. *Heat Mass Transf.* 2017;53:265–75.
 72. Fang J, Xuan Y. Investigation of optical absorption and photo-thermal conversion characteristics of binary CuO/ZnO nanofluids. *RSC Adv.* 2017;7(88):56023–33.
 73. Duangthongsuk W, Wongwises S. Measurement of temperature-dependent thermal conductivity and viscosity of TiO₂-water nanofluids. *Exp Therm Fluid Sci.* 2009;33:706–14. <https://doi.org/10.1016/j.expthermflusci.2009.01.005>.
 74. Hwang Y, Lee JK, Lee JK, Jeong YM, Cheong SI, Ahn YC, Kim SH. Production and dispersion stability of nanoparticles in nanofluids. *Powder Technol.* 2008;186(2):145–53.
 75. Aglawe KR, Yadav RK, Thool SB. Preparation, applications and challenges of nanofluids in electronic cooling: a systematic review. *Mater Today Proc.* 2021;43:366–72. <https://doi.org/10.1016/j.matpr.2020.11.679>.
 76. Feng X, Ma H, Huang S, Pan W, Zhang X, Tian F, Luo J. Aqueous– organic phase-transfer of highly stable gold, silver, and platinum nanoparticles and new route for fabrication of gold Nanofilms at the oil/water Interface and on solid supports. *J Phys Chem B.* 2006;110(25):12311–7.
 77. Jiang W, Song J, Jia T, Yang L, Li S, Li Y, et al. A comprehensive review on the pre-research of nanofluids in absorption refrigeration systems. *Energy Rep.* 2022;8:3437–65. <https://doi.org/10.1016/j.egy.2022.02.087>.
 78. Xuan Y, Li Q, Hu W. Aggregation structure and thermal conductivity of nanofluids. *AIChE J.* 2003;49(4):1038–43.
 79. Popa I, Gillies G, Papastavrou G, Borkovec M. Attractive and repulsive electrostatic forces between positively charged latex particles in the presence of anionic linear polyelectrolytes. *J Phys Chem B.* 2010;114(9):3170–7.
 80. Rubbi F, Das L, Habib K, Aslfattahi N, Saidur R. State-of-the-art review on water-based nanofluids for low temperature solar thermal collector application. *Sol Energy Mater Sol Cells.* 2021;230:111220. <https://doi.org/10.1016/j.solmat.2021.111220>.
 81. Chakraborty S, Panigrahi PK. Stability of nanofluid: A review. *Appl Therm Eng.* 2020;174:115259.
 82. Zhang H, Qing S, Zhai Y, Zhang X, Zhang A. The changes induced by pH in TiO₂/water nanofluids: stability, thermophysical properties and thermal performance. *Powder Technol.* 2021;377:748–59.
 83. Wang X, Zhu D. Investigation of pH and SDBS on enhancement of thermal conductivity in nanofluids. *Chem Phys Lett.* 2009;470:107–11. <https://doi.org/10.1016/j.cplett.2009.01.035>.
 84. Rajesh C, Deepak K, Aditya K, Sudhakar S. Stability analysis of Al₂O₃/water nanofluids. *J Exp Nanosci.* 2017;12(1):140–51. <https://doi.org/10.1080/17458080.2017.1285445>.
 85. Jong T, Pil S, Kedzierski MA. Effect of surfactants on the stability and solar thermal absorption characteristics of water-based nanofluids with multi-walled carbon nanotubes. *Int J Heat Mass Transf.* 2018;122:483–90. <https://doi.org/10.1016/j.ijheatmasstransfer.2018.01.141>.
 86. Vold MJ. Van der Waals' attraction between anisometric particles. *J Colloid Sci.* 1954;9:451–9.
 87. Kim HJ, Lee SH, Lee JH, Jang SP. Effect of particle shape on suspension stability and thermal conductivities of water-based bohemite alumina nanofluids. *Energy.* 2015;90:1290–7.
 88. Chakraborty S, Sarkar I, Ashok A, Sengupta I, Pal SK. Thermophysical properties of Cu-Zn-Al LDH nano fluid and its application in spray cooling. *Appl Therm Eng.* 2018;141:339–51. <https://doi.org/10.1016/j.applthermaleng.2018.05.114>.
 89. Yazid MNAWM, Sidik NAC, Mamat R, Najafi G. A review of the impact of preparation on stability of carbon nanotube nanofluids. *Int Commun Heat Mass Transf.* 2016;78:253–63.
 90. Sami W, Amiri A, Kazi SN, Badarudin A. Stability and thermophysical properties of non-covalently functionalized graphene nanoplatelets nanofluids. *Energy Convers Manage.* 2016;116:101–11. <https://doi.org/10.1016/j.enconman.2016.02.082>.
 91. Li Y, Tung S, Schneider E, Xi S. A review on development of nanofluid preparation and characterization. *Powder Technol.* 2009;196(2):89–101.
 92. LotfizadehDehkordi B, Kazi SN, Hamdi M, Ghadimi A, Sadeghinezhad E, Metselaar HSC. Investigation of viscosity and thermal conductivity of alumina nanofluids with addition of SDBS. *Heat Mass Transf.* 2013;49(8):1109–15.
 93. Nikkha V, Sarafraz MM, Hormozi F, Peyghambarzadeh SM. Particulate fouling of CuO – water nanofluid at isothermal diffusive condition inside the conventional heat

- exchanger-experimental and modeling. *Exp Therm Fluid Sci.* 2015;60:83–95. <https://doi.org/10.1016/j.expthermflusci.2014.08.009>.
94. Singh V, Kumar A, Alam M, Kumar A, Kumar P, Goyat V. A study of morphology UV measurements and zeta potential of Zinc Ferrite and Al₂O₃ nanofluids. *Mater Today Proc.* 2022. <https://doi.org/10.1016/j.matpr.2022.02.371>.
 95. Shazali SS, Amiri A, Zubir MNM, Rozali S, Zabri MZ, Sabri MFM, Soleymaniha M. Investigation of the thermophysical properties and stability performance of non-covalently functionalized graphene nanoplatelets with Pluronic P-123 in different solvents. *Mater Chem Phys.* 2018;206:94–102.
 96. Almanassra IW, Manasrah AD, Al-mubaiyedh UA, Al-ansari T. An experimental study on stability and thermal conductivity of water / CNTs nano fluids using different surfactants : a comparison study. *J Mol Liq.* 2020;304:111025. <https://doi.org/10.1016/j.molliq.2019.111025>.
 97. Kim HJ, Bang IC, Onoe J. Characteristic stability of bare Au-water nanofluids fabricated by pulsed laser ablation in liquids. *Opt Lasers Eng.* 2009;47(5):532–8.
 98. Chamsa-Ard W, Brundavanam S, Fung CC, Fawcett D, Poinern G. Nanofluid types, their synthesis, properties and incorporation in direct solar thermal collectors: a review. *Nanomaterials.* 2017;7(6):131.
 99. Anushree C, Philip J. Assessment of long term stability of aqueous nano fluids using different experimental techniques. *J Mol Liq.* 2016;222:350–8. <https://doi.org/10.1016/j.molliq.2016.07.051>.
 100. Gallego A, Cacua K, Herrera B, Cabaleiro D, Piñeiro MM, Lugo L. Experimental evaluation of the effect in the stability and thermophysical properties of water-Al₂O₃ based nanofluids using SDBS as dispersant agent. *Adv Powder Technol.* 2020;31:560–70. <https://doi.org/10.1016/j.apt.2019.11.012>.
 101. Chakraborty S, Sarkar I, Behera DK, Pal SK, Chakraborty S. Experimental investigation on the effect of dispersant addition on thermal and rheological characteristics of TiO₂ nanofluid. *Powder Technol.* 2017;307:10–24.
 102. Ghadimi A, Saidur R, Metselaar HSC. A review of nanofluid stability properties and characterization in stationary conditions. *Int J Heat Mass Transf.* 2011;54:4051–68. <https://doi.org/10.1016/j.ijheatmasstransfer.2011.04.014>.
 103. Ilyas SU, Pendyala R, Narahari M. Stability and thermal analysis of MWCNT-thermal oil-based nano fluids. *Colloids Surf A.* 2017;527:11–22. <https://doi.org/10.1016/j.colsurfa.2017.05.004>.
 104. Chakraborty S, Sengupta I, Sarkar I, Pal SK, Chakraborty S. Effect of surfactant on thermo-physical properties and spray cooling heat transfer performance of Cu-Zn-Al LDH nanofluid. *Appl Clay Sci.* 2019;168:43–55. <https://doi.org/10.1016/j.clay.2018.10.018>.
 105. Said Z, Hachicha AA, Aberoumand S, Yousef BA, Sayed ET, Bellos E. Recent advances on nanofluids for low to medium temperature solar collectors: energy, exergy, economic analysis and environmental impact. *Prog Energy Combust Sci.* 2021;84:100898.
 106. Yılmaz İH, Mwesigye A. Modeling, simulation and performance analysis of parabolic trough solar collectors: a comprehensive review. *Appl Energy.* 2018;225:135–74.
 107. Hu X, Li Y, Tian J, Yang H, Cui H. Highly efficient full solar spectrum (UV- [9 _ TD \$ IF] vis-NIR) photocatalytic performance of Ag₂S quantum dot / TiO₂ nanobelt heterostructures. *J Ind Eng Chem.* 2017;45:189–96. <https://doi.org/10.1016/j.jiec.2016.09.022>.
 108. Sajid MU, Bicer Y. Nanofluids as solar spectrum splitters: a critical review. *Sol Energy.* 2020;207:974–1001. <https://doi.org/10.1016/j.solener.2020.07.009>.
 109. Han D, Meng Z, Wu D, Zhang C, Zhu H. Thermal properties of carbon black aqueous nanofluids for solar absorption. *Nanoscale Res Lett.* 2011;6(1):1–7.
 110. Walshe J, Amarandei G, Ahmed H, McCormack S, Doran J. Development of poly-vinyl alcohol stabilized silver nanofluids for solar thermal applications. *Sol Energy Mater Sol Cells.* 2019;201:110085. <https://doi.org/10.1016/j.solmat.2019.110085>.
 111. Chen M, He Y, Ye Q, Wang X, Hu Y. Shape-dependent solar thermal conversion properties of plasmonic Au nanoparticles under different light filter conditions. *Sol Energy.* 2019;182:340–7. <https://doi.org/10.1016/j.solener.2019.02.070>.
 112. Fang J, Zhang P, Chang H, Wang X. Hydrothermal synthesis of nanostructured CuS for broadband efficient optical absorption and high-performance photo-thermal conversion. *Sol Energy Mater Sol Cells.* 2018;185:456–63. <https://doi.org/10.1016/j.solmat.2018.05.060>.
 113. Subramanian AL, Priya SL, Kottaisamy M, Ilangoan R. Investigations on the absorption spectrum of TiO₂ nanofluid. *J Energy South Afr.* 2014;25(4):123–7.
 114. Khullar V, Bhalla V, Tyagi H. Potential heat transfer fluids (nanofluids) for direct volumetric absorption-based solar thermal systems. *J Therm Sci Eng Appl.* 2018;10(1):011009.
 115. Shende R, Sundara R. Nitrogen doped hybrid carbon based composite dispersed nano fluids as working fluid for low-temperature direct absorption solar collectors. *Sol Energy Mater Sol Cells.* 2015;140:9–16. <https://doi.org/10.1016/j.solmat.2015.03.012>.
 116. Lee S, Jang SP. Extinction coefficient of aqueous nanofluids containing multi-walled carbon nanotubes. *Int J Heat Mass Transf.* 2013;67:930–5. <https://doi.org/10.1016/j.ijheatmasstransfer.2013.08.094>.
 117. An W, Chen L, Liu T, Qin Y. Enhanced solar distillation by nanofluid-based spectral splitting PV/T technique: preliminary experiment. *Sol Energy.* 2018;176:146–56.
 118. Zeiny A, Jin H, Bai L, Lin G, Wen D. A comparative study of direct absorption nano fluids for solar thermal applications. *Sol Energy.* 2018;161:74–82. <https://doi.org/10.1016/j.solener.2017.12.037>.
 119. He Y, Chen M, Wang X, Hu Y. Plasmonic multi-thorny Gold nanostructures for enhanced solar thermal conversion. *Sol Energy.* 2018;171:73–82. <https://doi.org/10.1016/j.solener.2018.06.071>.
 120. Said Z, Saidur R, Rahim NA. Optical properties of metal oxides based nano fluids ☆. *Int Commun Heat Mass Transf.* 2014;59:46–54. <https://doi.org/10.1016/j.icheatmasstransfer.2014.10.010>.
 121. Zhu Q, Cui Y, Mu L, Tang L. Characterization of thermal radiative properties of nanofluids for selective absorption of solar radiation. *Int J Thermophys.* 2013;34(12):2307–21.
 122. Koblinski P, Phillpot SR, Choi SUS, Eastman JA. Mechanisms of heat flow in suspensions of nano-sized particles (nanofluids). *Int J Heat and Mass Transf.* 2002;45(4):855–63.
 123. Sabiha MA, Mostafizur RM, Saidur R, Mekhilef S. Experimental investigation on thermo physical properties of single walled carbon nanotube nanofluids. *Int J Heat Mass Transf.* 2016;93:862–71. <https://doi.org/10.1016/j.ijheatmasstransfer.2015.10.071>.
 124. Omrani AN, Esmaeilzadeh E, Jafari M, Behzadmehr A. Effects of multi walled carbon nanotubes shape and size on thermal conductivity and viscosity of nanofluids. *Diam Relat Mater.* 2019;93:96–104. <https://doi.org/10.1016/j.diamond.2019.02.002>.
 125. Wang L, Zhu G, Wang M, Yu W, Zeng J, Yu X, Li Q. Dual plasmonic Au/TiN nanofluids for efficient solar photothermal conversion. *Sol Energy.* 2019;184:240–8.
 126. Chen W, Zou C, Li X. Application of large-scale prepared MWCNTs nanofluids in solar energy system as volumetric solar absorber. *Sol Energy Mater Sol Cells.* 2019;200:109931. <https://doi.org/10.1016/j.solmat.2019.109931>.

127. Wang D, Jia Y, He Y, Wang L, Fan J, Xie H, et al. Enhanced photothermal conversion properties of magnetic nanofluids through rotating magnetic field for direct absorption solar collector. *J Colloid Interface Sci.* 2019;557:266–75. <https://doi.org/10.1016/j.jcis.2019.09.022>.
128. Mehrali M, Krishna M, Pecnik R. Full-spectrum volumetric solar thermal conversion via graphene / silver hybrid plasmonic nanofluids. *Appl Energy.* 2018;224:103–15. <https://doi.org/10.1016/j.apenergy.2018.04.065>.
129. Heyhat MM, Valizade M, Abdolazade S, Maerefat M. Thermal efficiency enhancement of direct absorption parabolic trough solar collector (DAPTSC) by using nanofluid and metal foam. *Energy.* 2020;192:116662. <https://doi.org/10.1016/j.energy.2019.116662>.
130. Tong Y, Chi X, Kang W, Cho H. Comparative investigation of efficiency sensitivity in a flat plate solar collector according to nanofluids. *Appl Therm Eng.* 2020;174:115346.
131. Choudhary S, Sachdeva A, Kumar P. Influence of stable zinc oxide nanofluid on thermal characteristics of flat plate solar collector. *Renew Energy.* 2020;152:1160–70. <https://doi.org/10.1016/j.renene.2020.01.142>.
132. Eltaweel M, Abdel-rehim AA. Energy and exergy analysis of a thermosiphon and forced-circulation flat-plate solar collector using MWCNT / Water nanofluid. *Case Stud Therm Eng.* 2019;14:100416. <https://doi.org/10.1016/j.csite.2019.100416>.
133. Hussein OA, Habib K, Muhsan AS, Saidur R, Alawi OA, Ibrahim TK. Thermal performance enhancement of a flat plate solar collector using hybrid nanofluid. *Sol Energy.* 2020;204:208–22. <https://doi.org/10.1016/j.solener.2020.04.034>.
134. Sajid M, Abid M, Muhammad H, Pervez K, Anser M, Javed S. Comparative performance assessment of solar dish assisted s-CO₂ Brayton cycle using nanofluids. *Appl Therm Eng.* 2019;148:295–306. <https://doi.org/10.1016/j.applthermaleng.2018.11.021>.
135. Potenza M, Milanese M, Colangelo G, De RA. Experimental investigation of transparent parabolic trough collector based on gas-phase nanofluid. *Appl Energy.* 2017;203:560–70. <https://doi.org/10.1016/j.apenergy.2017.06.075>.
136. Lee SH, Choi TJ, Jang SP. Thermal efficiency comparison: Surface-based solar receivers with conventional fluids and volumetric solar receivers with nanofluids. *Energy.* 2016;115:404–17.
137. Yang L, Du K. Thermo-economic analysis of a novel parabolic trough solar collector equipped with preheating system and canopy. *Energy.* 2020;211:118900. <https://doi.org/10.1016/j.energy.2020.118900>.
138. Fan M, Liang H, You S, Zhang H, Zheng W. Heat transfer analysis of a new volumetric based receiver for parabolic trough solar collector. *Energy.* 2018;142:920–31. <https://doi.org/10.1016/j.energy.2017.10.076>.
139. Abid M, Ratlamwala TAH, Atikol U. ScienceDirect Solar assisted multi-generation system using nanofluids: a comparative analysis. *Int J Hydrog Energy.* 2017;42:21429–42. <https://doi.org/10.1016/j.ijhydene.2017.05.178>.
140. Choudhary S, Sachdeva A, Kumar P. Investigation of the stability of MgO nanofluid and its effect on the thermal performance of flat plate solar collector. *Renew Energy.* 2020;147:1801–14. <https://doi.org/10.1016/j.renene.2019.09.126>.
141. Yang L, Ji W, Mao M, Huang J. An updated review on the properties, fabrication and application of hybrid-nanofluids along with their environmental effects. *J Clean Prod.* 2020;257:120408. <https://doi.org/10.1016/j.jclepro.2020.120408>.

Publisher's Note Springer Nature remains neutral with regard to jurisdictional claims in published maps and institutional affiliations.

Springer Nature or its licensor (e.g. a society or other partner) holds exclusive rights to this article under a publishing agreement with the author(s) or other rightsholder(s); author self-archiving of the accepted manuscript version of this article is solely governed by the terms of such publishing agreement and applicable law.